Université d'Ottawa · University of Ottawa

Time Domain Equalizer Design Based on Multi-rate Technique

By

Yong Yu

A thesis submitted to
The School of Graduate Studies and Research
University of Ottawa
In partial fulfillment of the requirements
For the degree of

Master of Science
In System Science

System Science Program
Faculty of Administration
University of Ottawa
Ottawa, Ontario, Canada

April 2002

Abstract

Discrete Multitone is adopted in Digital Subscriber Line to offer high-speed data communication on the UTP channel. To combat the channel distortion, DMT system employed Time Domain Equalizer and Cyclic Prefix. In this thesis, we analyze different existing time domain equalizer design methods and their performances are compared based on our simulation results. Modification of the current method is proposed and significant performance improvement is obtained. Multi-rate equalization is studied theoretically, which enables us to achieve zero ISI channels that can be used not only in DMT system but also in all other communication systems. Our simulation results show that the new design method is superior and practical.

Acknowledgment

First of All, I would like to express the deepest thanks to my thesis supervisor, Dr. Tet H. Yeap, for his guidance and encouragement during the course of my M. Sc. Program.

Thanks to Dr. J. M. Thizy, my program director, who provide constant help and support on my graduate study.

Special thanks to my parents who bring me to this fantastic world and always support me in the world.

I extend a special thanks to my sister, Feng Yu, for her delicious foods and my girl friend, Cathy, for the happiness she brings to me.

Contents

Chapter 1 Introduction 1

1.1 Preliminaries 1

1.2 Thesis Objectives 4

1.3 Thesis Organization 4

1.4 Contributions 5

Chapter 2 Background 6

2.1 The Unshielded Twisted Pairs (UTP) Channel 6

2.2 Noise on the UTP channel 9

2.2.1 Crosstalk Noise 9

2.2.2 Bridge Taps 11

2.2.3 Impulse Noise 12

2.3 Discrete Multitone Modulation 12

2.3.1 Discrete Multitone Modulation 12

2.3.2 Water Pouring and Bit Loading 15

2.4 Intersymbol Interference and Interchannel Interference 18

2.5 Guard Time and Cyclic Prefix 19

2.6 Summary 21

Chapter 3 Current TEQ Design Methods 22

3.1 TEQ Design Criterions 22

3.2 Minimum Mean Square Error Method 23

3.3 Maximum Shorten SNR Method 26

3.4 Geometric TEQ Method 28

3.5 Summary 30

Chapter 4 Proposed TEQ Design Methods 31
4.1 Modified MMSE Method 31
4.2 Multirate Time Domain Equalizer Design 34
4.3 Multirate Zero ISI (MRZISI) TEQ Design 40
4.4 Discussion of Noise Effect 41
4.5 Complexity Comparison of the TEQ Design Methods 43
4.6 Additional Remarks 45

Chapter 5 Simulation Results 47
5.1 Simulation Results of MMSE Method 47
5.2 Simulation Results of Modified MMSE Method 53
5.3 Simulation Results of MSSNR Method 56
5.4 Simulation Results of MRZISI Design Method 60
5.5 Comparison of the Simulation Results with Accurate Channel Information 68
5.6 Simulation Results with Estimated Channel Information 71
5.7 Additional Remarks on SSNR and ISI Shaping 74

Chapter 6 Conclusions and Future Works 78

Reference 80

List of Figures

Figure 1.1 Frequency Response of a Typical UTP Channel 1
Figure 1.2 Magnitude Response of One Sub-channel 3
Figure 1.3 Different Kinds of Interference 3

Figure 2.1 UTP Line Model 7
Figure 2.2 Impulse and Frequency Response of an Idea Channel 7
Figure 2.3 CSA Loop4 Structure 8
Figure 2.4 Impulse Response of CSALoop4 8
Figure 2.5 Frequency Response of CSALoop4 8
Figure 2.6 Crosstalks 9
Figure 2.7 Ratio of FEXT Power to Signal Power 11
Figure 2.8 Sub-channels of G.lite and G.dmt 13
Figure 2.9 DMT Transmitter and Receiver 13
Figure 2.10 The Optimum Power Distribution Based on Water Pouring 16
Figure 2.11 Interference 18
Figure 2.12 Cyclic Prefix 19
Figure 2.13 Revised System Diagram 20

Figure 3.1 MMSE TEQ Design Structure 23

Figure 4.1 Target Impulse Response 32
Figure 4.2 MSE Distribution 32
Figure 4.3 Revised System Diagram 36
Figure 4.4 Channel Impulse Response of CSALoop1 38
Figure 4.5 Multirate TEQ 39
Figure 4.6 Shortened Channel Impulse Response 39

Figure 5.1 Achieved Bit Rate of MMSE TEQ with Different Length 48

Figure 5.2 Channel Impulse Response of CSALoop 2 48
Figure 5.3 TEQ Taps Designed with MMSE Method 49
Figure 5.4 Shortened Channel Impulse Response with MMSE Method 49
Figure 5.5 Shortened Channel Frequency Response with MMSE Method 50
Figure 5.6 Channel Impulse Response of CSALoop 7 50
Figure 5.7 TEQ Designed with MMSE Method 51
Figure 5.8 Shortened Channel with MMSE Method 51
Figure 5.9 Shortened Channel Frequency Response with MMSE Method 52
Figure 5.10 Achieved Bit Rate of MMSE Method 52
Figure 5.11 TEQ designed by Modified MMSE Method 53
Figure 5.12 Shortened Impulse Response 54
Figure 5.13 Frequency Response of the Shortened Channel 54
Figure 5.14 Bit Loading Result 55
Figure 5.15 TEQ and Shortened Channel Impulse response 55
Figure 5.16 Achieved Bit Rate of Modified MMSE Method 56
Figure 5.17 TEQ Taps Designed with MSSNR Method 57
Figure 5.18 Shortened Channel Impulse Response with MSSNR Method 57
Figure 5.19 Shortened Channel Frequency Response with MSSNR Method 58
Figure 5.20 TEQ Designed with MSSNR Method 59
Figure 5.21 Shortened Channel with MSSNR Method 59
Figure 5.22 Achieved Bit Rate of MSSNR Method 60
Figure 5.23 Channel Impulse Response of CSALoop 3 61
Figure 5.24 TEQ Designed with MRZISI Method 61
Figure 5.25 Impulse Response of the Shortened Channel 62
Figure 5.26 Frequency Response of the Shortened Channel 62
Figure 5.27 Truncated TEQ Taps 63
Figure 5.28 Impulse Response of Shortened Channel 64
Figure 5.29 Frequency Response of Shortened Channel 64
Figure 5.30 Truncated TEQ Taps 65
Figure 5.31 Impulse Response of Shortened Channel 65
Figure 5.32 Frequency Response of Shortened Channel 66

Figure 5.33 Bit Loading Result 66
Figure 5.34 Achieved Bit Rate of MRZISI Method 67
Figure 5.35 Achieved SSNR with Different Delay 67
Figure 5.36 Comparison of Achieved Bit Rate of Different Methods 69
Figure 5.37 Actual and Estimated Channel Impulse Response 72
Figure 5.38 Comparison of Achieved Bit Rate of Different Methods 73
Figure 5.39 Shortened Impulse Response with Accurate Channel Information 74
Figure 5.40 Shortened Impulse Response with Estimated Channel Information 75
Figure 5.41 Bit Loading Result in Case 1 75
Figure 5.42 Bit Loading Result in Case 2 76
Figure 5.43 ISI and Signal Spectrum in Case 1 76
Figure 5.44 ISI and Signal Spectrum in Case 2 77

List of Tables

Table 4-1 MMSE Computational Complexity 43
Table 4-2 MSSNR Computational Complexity 43
Table 4-3 MRZISI Computational Complexity 44
Table 4-4 Comparison of Computational Complexity 44

Table 5-1 SSNR of Different Methods 68
Table 5-2 Transmission Rate (kbps) 69
Table 5-3 Comparisons of Different Methods with Different CP Length 70

Glossary

ADC	Analog to Digital Converter
ADSL	Asymmetric Digital Subscriber Line
AWGN	Addictive White Gaussian Noise
CO	Central Office
CP	Cyclic Prefix
DAC	Digital to Analog Converter
DMT	Discrete MultiTone
DSL	Digital Subscriber Line
FEXT	Far-End Crosstalk
FFT	Fast Fourier Transform
ICI	Inter Channel Interference
IFFT	Inverse Fast Fourier Transform
ISCI	Inter Symbol Inter Channel Interference
ISI	Inter Symbol Interference
MMSE	Minimum Mean Square Error
MSSNR	Maximum Shorten SNR
NEXT	Near-End Crosstalk
PSD	Power Spectral Density
PSTN	Public Switched Telephone Network
QAM	Quadrature Amplitude Modulation
SNR	Signal to Noise Ratio
SSNR	Shortening Signal to Noise Ratio
TEQ	Time Domain Equalizer
TIR	Target Impulse Response
UTP	Unshielded Twist Pair
UEC	Unit Energy Constraint
UTC	Unit Tap Constraint

Chapter 1

Introduction

1.1 Preliminaries

The demand for residential broadband services required to provide high-speed, interactive and two-way connections has been growing explosively. Digital subscriber line (DSL) technologies use the existing unshielded twisted paired lines (UTP) to reach most of the customers to provide cost-effective, dedicated and uninterrupted high data rate connections that are secure and are always on.

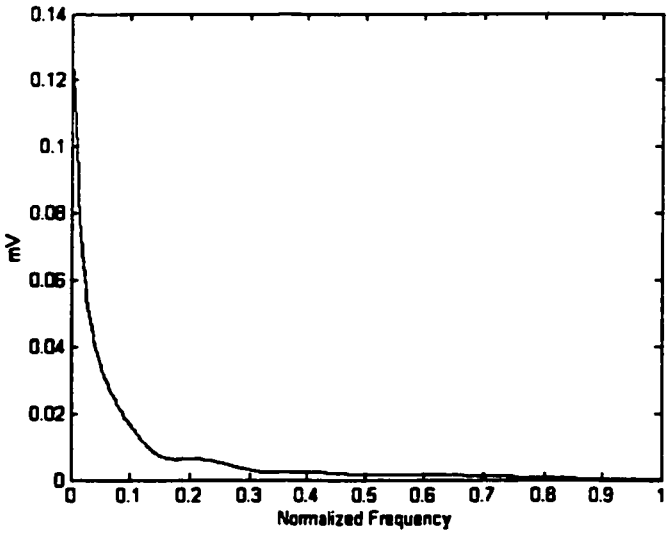

Figure 1.1 Frequency Response of a Typical UTP Channel

Unfortunately, the UTP channel is not designed for high-speed data communication but rather for low frequency analog voice transmission. Its gain and phase vary greatly with the change of the frequency, which lead to severe signal attenuation and distortion. The frequency response of a typical UTP channel is given in Figure 1.1. Besides the channel attenuation and distortion, different kinds of noises also impair the signal on UTP channel especially crosstalk noise. Crosstalk noise refers simply to the disturbance on one twisted pair due to signals on other twisted pairs in the same UTP bundle.

To transmit high-speed data on a UTP channel, either single carrier modulation technique or multi-carrier modulation technique can be used. Multi-carrier modulation technique has been demonstrated to be optimal if the number of the sub-channel is large [5]. In a DSL system, Discrete Multitone (DMT) was adopted as the standard multi carrier modulation technique.

Discrete Multitone divides the total usable bandwidth into a large number of sub channels and if each sub channel is narrow enough, the frequency response of the sub channel can be regarded as ideal. On each sub-channel, M-QAM is used as the modulation method and M depends on the signal to noise ratio (SNR) of the sub channel, which can be estimated at system startup.

In practice, the bandwidth of each sub channel cannot be zero. This means that the channel gain and phase still vary within each sub channel. Figure 1.2 shows the channel gain of one sub channel.

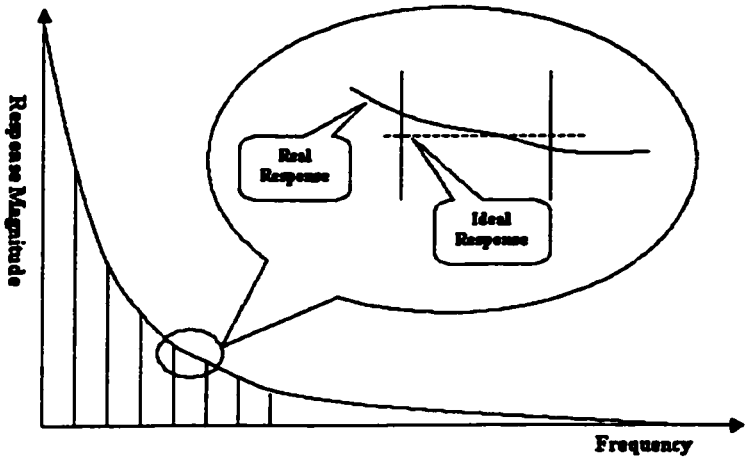

Figure 1.2 Magnitude Response of One Sub-channel

Such variation in each sub-channel is small but still causes different kinds of signal interferences such as intersymbol interference (ISI), interchannel interference (ICI) and intersymbol interchannel interference (ISCI) which are illustrated in Figure 1.3.

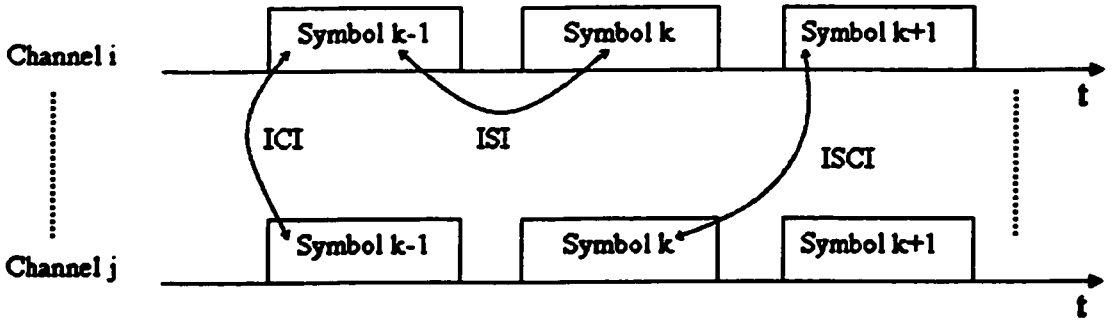

Figure 1.3 Different Kinds of Interference

To deal with such interference, DSL system uses a Cyclic Prefix (CP), which is inserted at the beginning of each transmission segment by copying the last N bits of the segment and putting them in front of the segment. If the length of the CP is greater than the length of the channel impulse response, no interference occurs. However the length of the CP cannot be too long because redundant bits are introduced causing lower system throughput. The problem we face is how to avoid the interference without significant decrease in the system throughput. This can be solved by using a Time Domain Equalizer

(TEQ) to shorten the channel impulse response so that a shorter CP can be used. The work in this thesis focuses on the design of such TEQ.

1.2 Thesis Objectives

In this thesis, two current TEQ design methods, Minimum Mean Square Error Method (MMSE) and Maximum Shorten SNR Method (MSSNR), are discussed and evaluated using Mat Lab simulation.

A modified TEQ design method based on MMSE method is proposed and its performance is compared with the current design methods.

Although the TEQ designed using the above methods could shorten the channel impulse response effectively, there is still some residual interference. A new design method, Multirate Zero ISI design method, which is based on the work of Ungerboeck on the design of optimum, multirate FIR filters for data transmission over ideal band-limited channels is proposed [42]. With multirate zero ISI design method, a zero ISI or near zero ISI channel can be achieved. This design method could be used not only as TEQ design method in DSL system but also be used in all other data transmission systems. Its feasibility and potential performance are examined through computer simulation.

1.3 Thesis Organization

In chapter 2, we introduce the UTP Channel and the principle of Discrete Multitone Modulation. Some key features of the DMT system and the effects of channel distortion are also introduced in this chapter. Current TEQ design methods are discussed in chapter 3. A modified design method and a new Multirate TEQ design method are presented in chapter 4. In chapter 5, the simulation results are given and different methods are compared. Conclusions and future enhancements are given in chapter 6.

1.4 Contributions

- Different TEQ design methods are simulated and comparisons are conducted based on the simulation results.

- The key features in the TEQ design and the criterions that the TEQ design should comply with are given.

- A modified MMSE design method is given and evaluated.

- A zero ISI filter design method is proposed and simulation is done to evaluate its performance.

- The proposed zero ISI filter design method is used to design TEQ and is compared to the other TEQ design methods.

Chapter 2

Background

On UTP channel, the channel gain and phase vary greatly with the change of frequency, which impair the signal carried by the channel. Multi carrier modulation has been demonstrated to be optimal on such channels if the number of the sub-channel is large enough [5]. Nevertheless, most early attempts to implement multi carrier modulation have failed because of the difficulties to find an efficient way to keep the equal distance between the adjacent carriers. By adopting IFFT/FFT as the modulation and demodulation method, DMT overcomes this problem successfully.

In this chapter, the UTP channel and the noises on UTP channel are introduced first. Then the general idea of DMT technique is presented and some key features are discussed.

2.1 The Unshielded Twisted Pairs (UTP) Channel

Unshielded Twisted Pairs have been widely used in the PSTN for more than one century. The UTP channel is appropriate for the transmission of the voice band signal occupying a bandwidth between 300Hz to 3400 Hz.

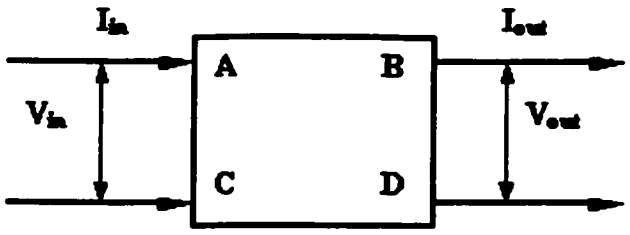

Figure 2.1 UTP Line Model

The UTP channel can be modeled as a two port networks, which can be described by parameters ABCD. These parameters reflect the voltage and current relationship between the input and the output.

$$\begin{aligned} V_{in} &= A \cdot V_{out} + B \cdot I_{out} \\ I_{in} &= C \cdot V_{out} + D \cdot I_{out} \end{aligned} \tag{2-1}$$

In this thesis, we are interested in the impulse and frequency responses of a UTP channel. An ideal physical channel has a flat frequency response and a direct delta impulse response which are shown in Figure 2.2.

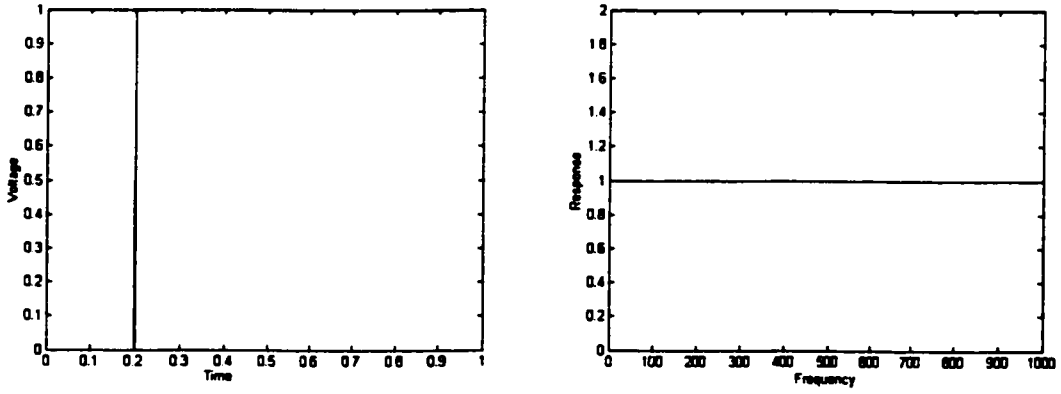

Figure 2.2 Impulse and Frequency Response of an Idea Channel

A real UTP channel has frequency dependent loss, which leads to channel attenuation and distortion. Figure 2.3 describes the structure of CSALoop4:

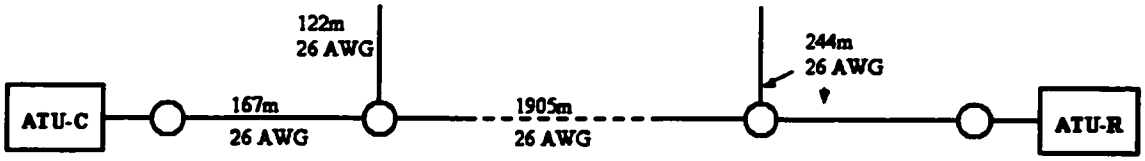

Figure 2.3 CSA Loop4 Structure

The impulse response and the frequency response of CSALoop4 are given in Figure 2.4 and Figure 2.5.

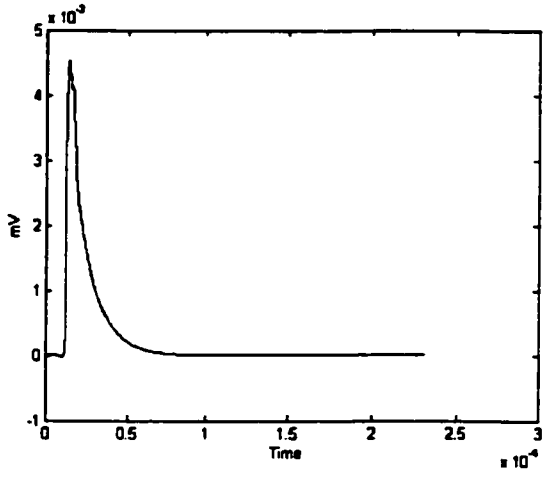

Figure 2.4 Impulse Response of CSALoop4

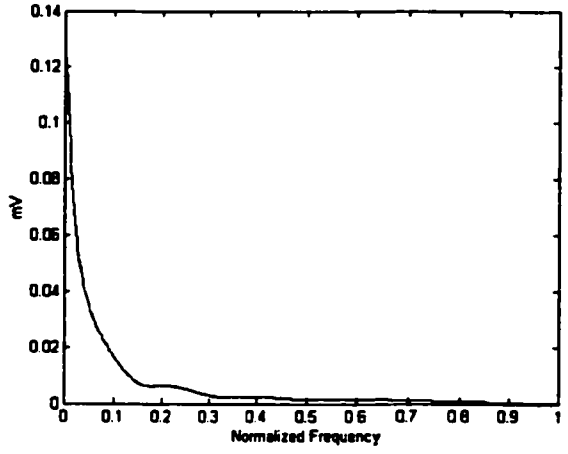

Figure 2.5 Frequency Response of CSALoop4

It can be observed that the frequency response of the UTP channel changes drastically and attenuates a lot on the high frequency band. Such a channel impairs the transmitted signal severely. Besides the channel distortion, the noise presented on the UTP channel also impairs the signal.

2.2 Noise on the UTP channel

Besides the channel attenuation and distortion, different kinds of noise also impair the signal on the UTP channel. In this section, we will briefly describe some noise sources on the UTP channel.

2.2.1 Crosstalk Noise

The UTP lines that connect end-users and COs (Central offices) are put into bundles. Crosstalk noise refers simply to the disturbance on one twisted pair due to signals on the other twisted pairs in the same bundle.

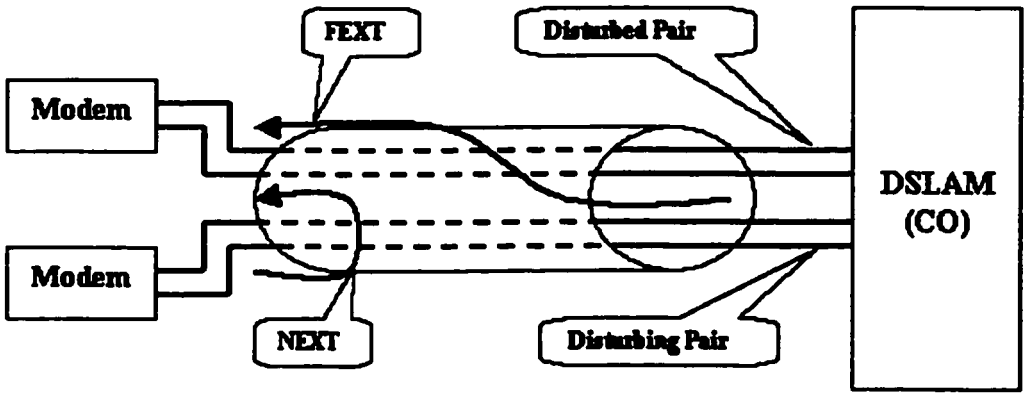

Figure 2.6 Crosstalks

Crosstalk is generally characterized either as near end Crosstalk (NEXT) or as far end Crosstalk (FEXT). NEXT appears on a loop at the same end of the cable as an interference source. In this case, the disturbing signal propagates down the disturbing twisted pair and couples into the disturbed pair's transmitter [6]. FEXT appears at the end of the cable opposite from the source of the interference. In this case, the disturbing signal propagates down the disturbing pair, couples into the disturbed pair's receiver. NEXT is usually the more severe of the two types, particularly at the central office, where there are many co-located transmitters. However, in ADSL, frequency-division multiplexing could drastically reduce the effect of NEXT. For this reason, NEXT is not considered in this thesis.

Far-end Crosstalk can be modeled by Equation 2-2. [13]

$$PSD_{FEXT} = PSD_{disturber} \cdot |H(f)|^2 \cdot K_{FEXT} \cdot \left(\frac{N}{49}\right)^{0.6} \cdot d \cdot f^2 \qquad (2\text{-}2)$$

where $H(f)$ is the channel's differential transfer function, K_{FEXT} is the FEXT coupling constant, N is the number of disturbers, d is the length of the loop in feet and f is the frequency in Hz.

We assume that both the signal and the disturbers have the same power spectral density, and then the PSD of the signal can be expressed as Equation 2-3.

$$PSD_{SIGNAL} = PSD_{disturber} \cdot |H(f)|^2 \qquad (2\text{-}3)$$

Therefore, the ratio of the FEXT power to the received information signal power can be written as Equation 2-4:

$$\frac{PSD_{FEXT}}{PSD_{SIGNAL}} = K_{FEXT} \cdot \left(\frac{N}{49}\right)^{0.6} \cdot d \cdot f^2 \qquad (2\text{-}4)$$

This ratio is shown in Figure 2.7 with the K_{FEXT} equal 6.36×10^{-19} and d equal 2000 feet. We could observe that the FEXT is about 40 dB less than the signal at the 1 MHz frequency point.

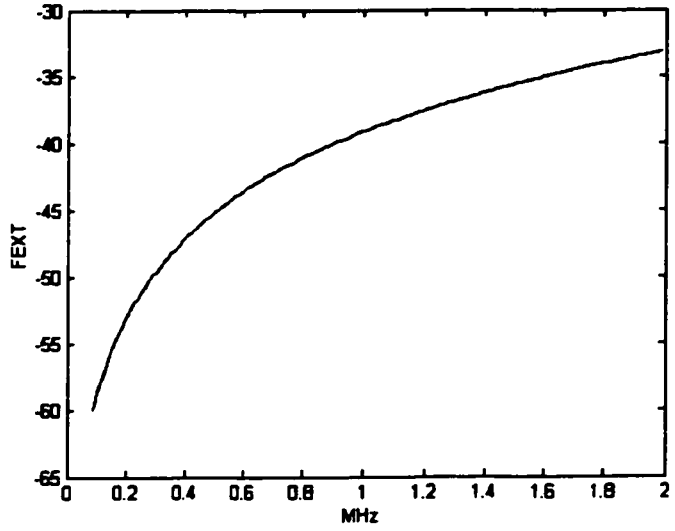

Figure 2.7 Ratio of FEXT Power to Signal Power

2.2.2 Bridge Taps

Existence of bridged taps is also one of the major impairments to high-speed transmission. A bridged tap is a piece of twisted pair wire that is connected to a loop at one end and is unterminated at the other end [7]. The bridged taps are usually connected in the splice cases; most of them are in underground installation. Approximately 80% of the loops in the United States have bridged taps and the major carriers cannot remove all the bridged taps because of the financial and labor cost.

Bridged taps have two principle effects on the transmitted signal. First, the bridged taps attenuate the signal; second, the transmitted signal is partially reflected at the unterminated end of the bridge tap and arrives at the receiver with a certain time of delay. Both effects decrease the signal noise ratio at the receiver end.

In the worst case, the delayed signal presents at the receiver 180° out of phase and partly cancelled the signal, causing an additional loss of 3 or 6 dB. The impacts of the bridged taps can be treated as in the echo cancellation, it is not considered in my thesis.

2.2.3 Impulse Noise

Impulse Noise can be generated both inside and outside the system such as the operation of the relay, the signaling in the adjacent loops. Typically the duration of the impulse noise is less than 1 ms [15, 16]. For peak voltage of the impulse noise between 5 and 40 mV, its distribution can be described as [20]:

$$P\{|v| > v_i\} = \left(\frac{5}{v_i}\right)^2 \tag{2-5}$$

2.3 Discrete Multitone Modulation

2.3.1 Discrete Multitone Modulation

Discrete Multitone (DMT) attracted considerable attentions as a practical and viable technology for high-speed data transmission over spectrally shaped noisy channel [5]. DMT is a kind of multi carrier modulation that superimposes several carrier-modulated waveforms to represent an input bit stream [4]. Unlike the conventional frequency division modulation, the number of transmitted bits on each sub-channel can be different in multi carrier modulation. The allocation algorithm of incoming bit stream to each sub channel which is called bit loading is crucial to the performance of DMT and is discussed later.

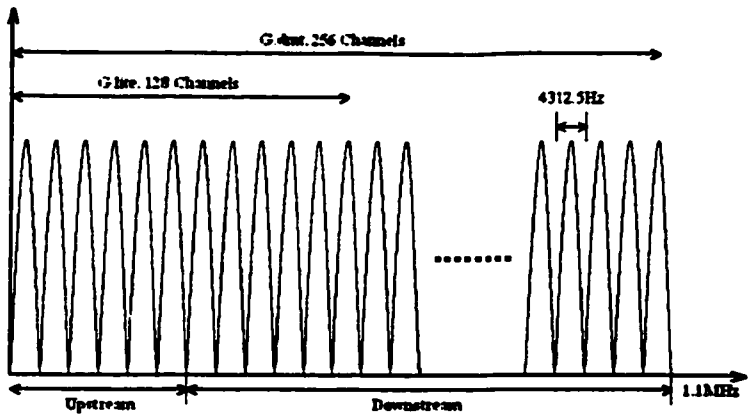

Figure 2.8 Sub-channels of G.lite and G.dmt

For G.dmt, DMT is a multi-carrier system with 256 carriers (or sub-channels) spaced 4.3125 kHz apart. G.lite uses less bandwidth than G.dmt, using only 128 channels to get bandwidth up to 552 kHz. G.lite systems feature the ability to coexist on the same wire with telephone service, without the installation of a special filter at the entrance to the home. Figure 2.8 illustrates the sub-channels used by G.lite and G.dmt. The diagram of a DMT transmitter/receiver is described in the Figure 2.9.

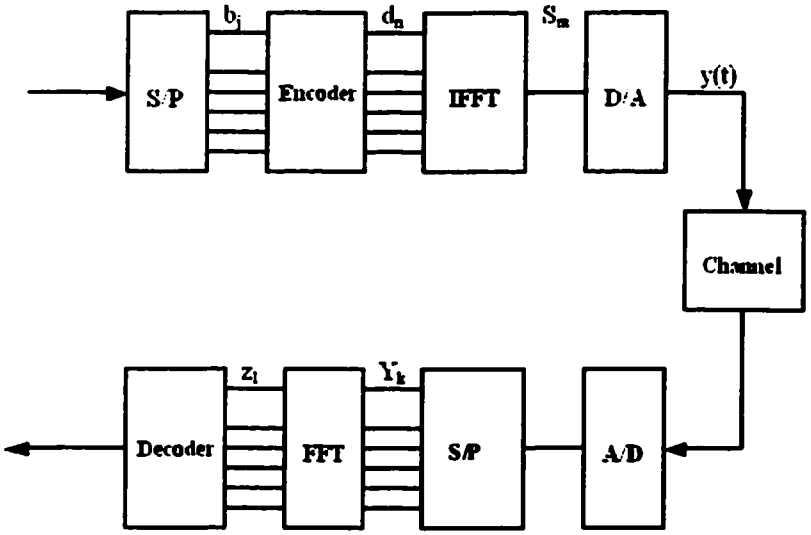

Figure 2.9 DMT Transmitter and Receiver

In the diagram, a serial bits stream is first converted into parallel bit stream and is assigned to different sub-channels based on the SNR of each sub-channel according to

the bit loading algorithm. The number of bits assigned to a particular sub-channel is represented by b_j.

Each of the b_j bits is mapped into a complex DMT sub-symbol d_n, where $d_n = a_n + b_n$. IFFT then performed on the vector $\{2d_n\}$, the result is a vector $S = \{S_0, S_1, \ldots, S_{n-1}\}$ of N complex numbers, with

$$S_m = \sum_{n=0}^{N-1} 2d_n e^{-j(2\pi nm/N)} = 2\sum_{n=0}^{N-1} d_n e^{-j2\pi f_n t_m} \tag{2-6}$$

where $f_n = \frac{n}{N \cdot \Delta t}$, $t_m = m \cdot \Delta t$, $m = 0,1,\cdots,N-1$ and Δt is an arbitrarily chosen interval. The real part of the vector S has components:

$$Y_m = 2\sum_{n=0}^{N-1}(a_n \cos 2\pi f_n t_m + b_n \sin 2\pi f_n t_m) \qquad m = 0,1,\cdots,N-1 \tag{2-7}$$

If these components are applied to a low-pass filter at time interval Δt, a signal is obtained that closely approximates the frequency-division multiplexed signal

$$y(t) = 2\sum_{n=0}^{N-1}(a_n \cos 2\pi f_n t + b_n \sin 2\pi f_n t) \qquad 0 \le t \le N \cdot \Delta t \tag{2-8}$$

Demodulation at the receiver is carried out via a Fast Fourier Transformation (FFT) of a vector of samples of the received signal. Since only the real part of the Fourier transform has been transmitted, it is necessary to sample twice as fast as expected, i.e., at intervals $\Delta t/2$. When there is no channel distortion, the receiver FFT operates on the 2N samples

$$Y_k = y\left(k\frac{\Delta t}{2}\right) = 2\sum_{n=0}^{N-1}\left(a_n \cos\frac{2\pi nk}{2N} + b_n \sin\frac{2\pi nk}{2N}\right) \qquad k = 0,1,\cdots,2N-1 \tag{2-9}$$

The FFT yields

$$z_i = \frac{1}{2N}\sum_{k=0}^{2N-1} Y_k e^{-j(2\pi ik/2N)} = \begin{cases} 2a_0, & i = 0 \\ a_i - jb_i, & i = 1,2,\cdots,N-1 \\ irrelevant, & i > N-1 \end{cases} \quad (2\text{-}10)$$

The original data a_i and b_i are available as the real and imaginary components of z_i. After pass the decoder, we then could recover the bits transmitted.

2.3.2 Water Pouring and Bit Loading

As we mentioned before, unlike the conventional frequency division modulation, the number of transmitted bits on each sub-channel can be different in multi carrier modulation. The algorithm that allocates transmitted bits onto each sub channel, called bit loading, is very crucial to the performance of DMT. In order to devise the bit-loading algorithm, we first introduce the water pouring method.

Recall that the Shannon limit of an ideal, band-limited, AWGN channel is:

$$C = W \cdot \log_2(1 + SNR) = W \cdot \log_2(1 + \frac{P_s}{W \cdot N_0}) \quad (2\text{-}11)$$

where C is the capacity in bits/s, W is the bandwidth and P_s is the transmitted power. In a DMT system, with Δf (bandwidth of the sub-channel) small enough, we could regard the sub-channel response |H(f)| as constant and the capacity of the sub-channel can be represented by [3]:

$$C_i = \Delta f \cdot \log_2\left[1 + \frac{\Delta f \cdot P(f_i) \cdot |H(f)|^2}{\Delta f \cdot N(f)}\right] \quad (2\text{-}12)$$

where $N(f)$ is the density of the noise power. The aggregate capacity across the whole band W is given by

$$C = \sum_i C_i = \int_W \log_2\left[1 + \frac{P(f)\cdot|H(f)|^2}{N(f)}\right] df \tag{2-13}$$

Under the constraint $P(f) > 0$ and $\int_W P(f)\,df \leq P_s$, to find the optimum transmit power spectrum $P(f)$ that maximizes C, we can use the Lagrange multiplier technique and maximize [6]

$$\log_2\left[1 + \frac{P(f)\cdot|H(f)|^2}{N(f)}\right] + \lambda \cdot P(f) \tag{2-14}$$

With respect to $P(f)$ where λ is a Lagrange multiplier. Continuing by differentiating gives

$$\frac{|H(f)|^2/N(f)}{1 + P(f)\cdot|H(f)|^2/N(f)} + \lambda = 0 \tag{2-15}$$

Equation 2-15 can be solved as

$$P(f) = K - N(f)/|H(f)|^2 \tag{2-16}$$

where K is a constant.

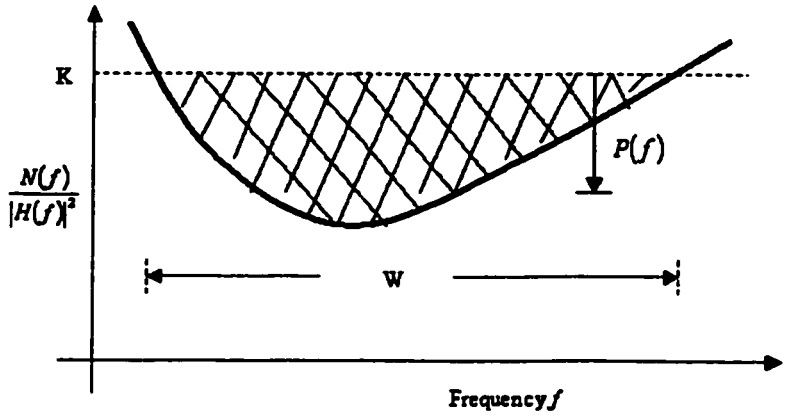

Figure 2.10 The Optimum Power Distribution Based on Water Pouring

The basic interpretation of the previous equation is that the signal power should be high when the channel SNR is high, and low when the channel SNR is low [10]. This result is called water-pouring algorithm and is illustrated in Figure 2.10.

Based on the water-pouring algorithm, we could devise the bit-loading algorithm. The number of the bits allocated to each sub-channel is based on the SNR of the sub-channel, From Equation 2-17, we could find that the carrier with higher SNR will be allocated more bits and the carrier with lower SNR will be allocated less bits,

$$b_j = \log_2\left(1+\frac{SNR_j}{\Gamma_{DMT}}\right) \tag{2-17}$$

where SNR_j is the output SNR of the j^{th} sub-channel and Γ_{DMT} is called the SNR gap defined by

$$\Gamma_{DMT} = \frac{d_{\min}^2}{12\cdot\sigma^2} \tag{2-18}$$

The number of the total bits transmitted per symbol is

$$b = \sum_j b_j = \sum_j \log_2\left[1+\frac{SNR_j}{\Gamma_{DMT}}\right] \tag{2-19}$$

The data rate that can be achieved is

$$R = \frac{b}{T} \tag{2-20}$$

where T is the duration of a symbol.

2.4 Intersymbol Interference and Interchannel Interference

In the previous section, we got the result of Equation 2-10 without considering the channel distortion. Considering the channel distortion, the result of the equation should be changed:

$$z_i = \frac{1}{2N}\sum_{k=0}^{2N-1} Y_k e^{-j(2\pi ik/2N)} = \frac{1}{2N}\sum_{k=0}^{2N-1}\left[2\sum_{n=0}^{N-1}\left(a_n \cos\frac{2\pi nk}{2N} + b_n \sin\frac{2\pi nk}{2N}\right)\right] e^{-j(2\pi ik/2N)} \tag{2-21}$$

If there is no channel distortion, the summation of all the components in the right of the equation with different k and different i will be zero. If distortion presents, the summation of all the components with different k and different i will not be zero, which is called interference.

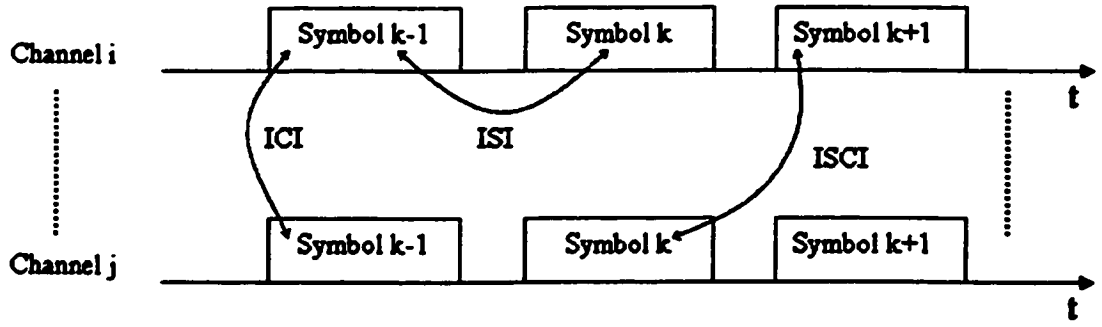

Figure 2.11 Interference

There are three kinds of interference: Intersymbol Interference, Interchannel Interference and Intersymbol Interchannel Interference. The Intersymbol Interference (ISI) is caused by the symbols in the same channel at different time (different k). This means, the previous symbols will influence the current symbol in the same channel. The Interchannel Interference (ICI) is caused by the symbols at the same time in different channels (different i). This means the current symbol in one channel will be influenced by the current symbols in the other channels. The Intersymbol Interchannel Interference (ISCI) is caused by the symbols at the different time in the different channels (different k

and i), which means the current symbol in one channel will be influenced by the previous symbols in other channels.

Presence of ISI, ICI and ISCI dramatically decreases the system performance. In the next section, we will introduce how to deal with all such kinds of interference in DSL system.

2.5 Guard Time and Cyclic Prefix

Due to the channel distortion, the orthogonality among sub-channels is destroyed and the interference presented. In order to deal with ISI, we adopt a blank guard time that is equal or longer than the length of the channel impulse response and is inserted between two adjacent transmitted symbols. With blank guard time, the ISI is eliminated but the ICI still exists. This is tackled by employing a cyclic prefix, commonly accepted as a means to mitigate ISI and preserve the orthogonality of the tones. The cyclic prefix is inserted at the start of each transmission segment by copying the last N bits of the segment and putting them in front of the segment as Figure 2.12 shows.

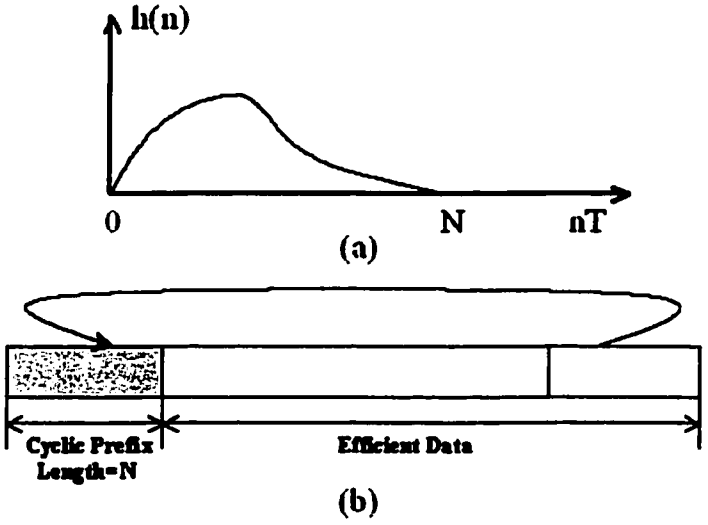

Figure 2.12 Cyclic Prefix

If the channel impulse response length is equal or shorter than N+1, the ISI and ICI can be avoided. The shortcoming of the cyclic prefix is obvious, redundant bits are

introduced and the bit rate is decreased. If the original block length is M, after adding the cyclic prefix, the efficiency of the transceiver is decreased by a factor of M/(N+M). In order to minimize the influence of the cyclic prefix, it is either desirable to make N as small as possible or utilize a large M. Increasing M increases the computation complexity, system delay, and memory requirements of the transceiver. To alleviate these problems, a time-domain FIR filter (TEQ) is typically placed in the receiver immediately following the A/D converter. The impulse response of the effective channel, which is the convolution of the TEQ and the physical channel, can be shortened compared to the impulse response of the original channel so that a shorter cyclic prefix can be adopted.

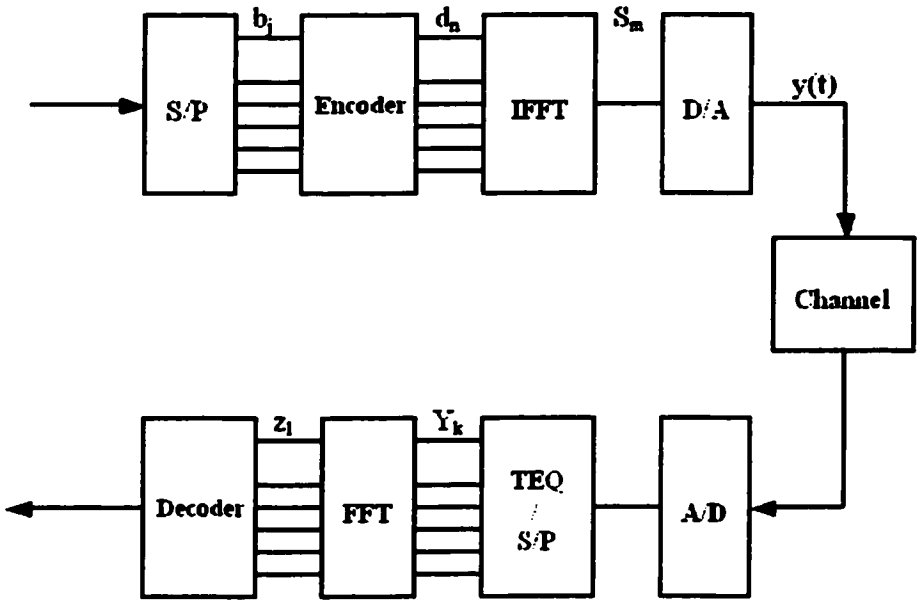

Figure 2.13 Revised System Diagram

In the next chapter, we present some current methods of designing the time domain equalizer.

2.6 Summary

The UTP channel poses serious impairments on the digital signal transmitted. Channel distortion and all kinds of noises such as FEXT, NEXT and AWGN severely deteriorate the performance of the high-speed data transmission system. Multi-carrier system is optimum in such kind of channel.

DMT is a kind of multi-carrier modulation method used in most xDSL systems. It could achieve high-speed data transmission on the UTP channel. To combat the channel distortion and channel noise, two elements are adopted, bit-loading algorithm and cyclic prefix. TEQ could shorten the channel impulse response effectively, which made a short cyclic prefix realizable.

Chapter 3

Current TEQ Design Methods

In order to use cyclic prefix to combat ISI and ICI resulted from channel attenuation and distortion, we first need to shorten the channel response so that the cyclic prefix can be adopted without decreasing the system throughput significantly. In this chapter, we first discuss some TEQ design criterions and then present some current design methods.

3.1 TEQ Design Criterions

The following remarks clarify some fundamental criterions in the TEQ design. Based on these criterions, we could tell whether a TEQ is good or not.

1. The TEQ should maximize the bit rate of the system. In order to maximize the transmission rate, the frequency response of the TEQ should have less or no nulls in the usable band since the sub-channels correspond to the nulls in the transmission band will surfer significant loss in their SNR and so does the number of bits allocated to them.

2. The delay of the TEQ cannot be extremely long since it will result in long delay in the system, which may nullify the system.

3. The TEQ cannot totally eliminate the ISI. How to deal with the ISI residue is a difficult problem. At present, this problem is not solved yet. Generally, we would like to put the residue to the band with lower SNR so that the influence on the overall system performance will be minimized.

4. A new parameter named Shortened Signal Noise ratio (SSNR) is widely used to evaluate the performance of the TEQ. SSNR is the ratio of the energy outside the window (Residue) to the energy inside the window. The higher the SSNR can be achieved, the better the performance of the TEQ.

3.2 Minimum Mean Square Error Method

Chow and Coiffi first employed channel-shortening equalization in multi-channel communication [49]. They used MMSE method to shorten the impulse response of a given channel to the length of the cyclic prefix, which is demonstrated in the Figure 3.1.

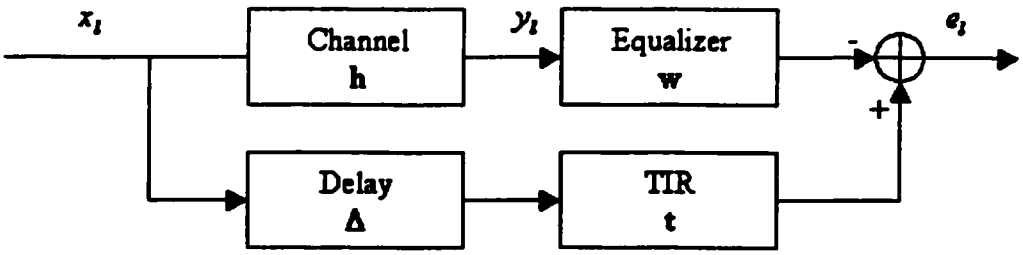

Figure 3.1 MMSE TEQ Design Structure

We set up the target impulse response (TIR) first. The goal of the MMSE method is to minimize the mean square error between the output of the TIR and the output of the equalizer. The effective channel impulse response c, which is the convolution of the physical channel response and the equalizer, would then be equal to a delayed version of

TIR. Thus changing the number of the taps of the TIR will force the effective channel impulse response to have the same length.

Assume that the length of the channel impulse response is L, we consider the output of the channel with block size N:

$$\begin{bmatrix} y_{k+N-1} \\ y_{k+N-2} \\ \vdots \\ y_k \end{bmatrix} = \begin{bmatrix} h_0 & \cdots & h_L & 0 & \cdots & 0 \\ 0 & h_0 & \cdots & h_L & 0 & \cdots \\ \vdots & \ddots & \ddots & \ddots & \ddots & \vdots \\ 0 & \cdots & 0 & h_0 & \cdots & h_L \end{bmatrix} \cdot \begin{bmatrix} x_{k+N-1} \\ x_{k+N-2} \\ \vdots \\ x_k \end{bmatrix} + \begin{bmatrix} n_{k+N-1} \\ n_{k+N-2} \\ \vdots \\ n_k \end{bmatrix} \tag{3-1}$$

In a more compact form:

$$y_k = Hx_k + n_k \tag{3-2}$$

The objective of MMSE is to minimize the mean square error (MSE) between outputs of the Equalizer and the TIR where MSE is expressed as

$$MSE = E\left(|e_k|^2\right) = E\left(e_k \cdot e_k^*\right) \tag{3-3}$$

where

$$e_k = t^T \cdot x_k - w^T \cdot y_k \tag{3-4}$$

so that

$$\begin{aligned} MSE &= E\left(\left(t^T \cdot x_k - w^T \cdot y_k\right) \cdot \left(t^T \cdot x_k - w^T \cdot y_k\right)^*\right) \\ &= t^T \cdot R_{xx} \cdot t - t^T \cdot R_{xy} \cdot w - w^T \cdot R_{yx} \cdot b + w^T \cdot R_{xx} \cdot w \end{aligned} \tag{3-5}$$

where $R_{xx} = E\left(x_k \cdot x_x^T\right)$, $R_{xy} = E\left(x_k \cdot y_x^T\right)$, $R_{yx} = E\left(y_k \cdot x_x^T\right)$ and $R_{yy} = E\left(y_k \cdot y_x^T\right)$. Since the optimal error sequence is uncorrelated with the observed data, we have

$$E\left(e_k \cdot y_k^*\right) = 0 \tag{3-6}$$

which means

$$t^T \cdot R_{xy} = w^T \cdot R_{yy} \tag{3-7}$$

With this equation, we could get

$$MSE = t^T \cdot \left[R_{xx} - R_{xy} \cdot R_{yy} \cdot R_{yx}\right] \cdot t = t^T \cdot R_{x|y} \cdot t \tag{3-8}$$

We define

$$S = \left[0_{(v+1)\times\Delta} \qquad I_{(v+1)\times(v+1)} \qquad 0_{(v+1)\times(N+L-\Delta-v-1)}\right]^T \tag{3-9}$$

where $v+1$ is the length of the TIR. Define

$$R_\Delta = S^T \cdot R_{x|y} \cdot S \tag{3-10}$$

the MSE can be written as

$$MSE = t^T \cdot R_\Delta \cdot t \tag{3-11}$$

Two constraints can be used here, one is unit-tap constraint (UTC) and the other is unit-energy constraint (UEC). Under the UTC constraint, Al-Dhahir and Cioffi define e_i as the i^{th} unit vector and form the Lagrangian

$$L^{UTC}(t,\lambda) = t^T \cdot R_\Delta \cdot t + \lambda \cdot \left(t^T \cdot e_i - 1\right) \tag{3-12}$$

Taking the gradient with respect to t and setting it to be zero

$$\frac{\partial L^{UTC}}{\partial t} = 2 \cdot R_\Delta \cdot t + \lambda \cdot e_i = 0 \tag{3-13}$$

which has the solution

$$t = \frac{R_\Delta^{-1} \cdot e_i}{R_\Delta^{-1}(i,i)} \tag{3-14}$$

where $i \in [0,v]$ and $R_\Delta^{-1}(i,i)$ is the i^{th} element in the diagonal of the matrix R_Δ^{-1}. From the solution of t, we get the MSE:

$$MSE = \frac{1}{R_\Delta^{-1}(i,i)} \tag{3-15}$$

The value of i that minimizes the MSE could be found by

$$i_{opt} = \arg\max_{0\le i\le v}\left\{R_\Delta^{-1}(i,i)\right\} \tag{3-16}$$

and the optimal t is given by

$$t_{opt} = \frac{R_\Delta^{-1} \cdot e_{iopt}}{R_\Delta^{-1}(i_{opt}, i_{opt})} \tag{3-17}$$

and w_{opt} can be obtained by using $t = t_{opt}$.

If the constraint of UEC is used, then the Lagrangian would become

$$L^{UEC}(t,\lambda) = t^T \cdot R_\Delta \cdot t + \lambda \cdot (t^T \cdot t - 1) \tag{3-18}$$

After setting the gradient of the above equation with respect to t to zero, we could get

$$R_\Delta \cdot t = \lambda \cdot t \tag{3-19}$$

From the above equation, we could find that t is an eigenvector of R_Δ. Since

$$MSE = t^T \cdot R_\Delta \cdot t = t^T \cdot \lambda \cdot t = \lambda \tag{3-20}$$

We should choose the eigenvector corresponding to the minimum eigenvalue of R_Δ to minimize the MSE.

The MMSE design method maximizes the SNR at the TEQ output [53]. The equalizer frequency response therefore tends to be a narrow band pass filter. The MMSE method does not have a mechanism to shape the residual ISI in frequency and there are deep notches in the frequency response of the designed TEQ.

3.3 Maximum Shorten SNR Method

Noticing that the TEQ design problem is actually a channel response shortening problem rather than an equalization problem, Melsa, Younce and Rohrs proposed a different solution: Maximum Shorten SNR method (MSSNR) [11]. Unlike MMSE method that maximizes the SNR of the TEQ output, the goal of MSSNR method is to find a TEQ that minimizes the energy of outside the target window while keeping the energy inside constant.

Let h to be the physical channel response with length L and w to be the TEQ with length M, so that the effective channel impulse response $c = h * w$ has a length of $L+M+1$. In order to shorten the channel impulse response, we would like to force as much as possible the channel response energy to lie in the $v+1$ consecutive samples, where v is the length of the cyclic prefix, and thus minimize the ISI. Let c_{win} represent a window of $v+1$ consecutive samples of c starting from the d^{th} sample and let c_{wall} represent the remaining $L+M-v-2$ samples. With these definitions,

$$c_{win} = \begin{bmatrix} c(d) \\ c(d+1) \\ \vdots \\ c(d+v) \end{bmatrix} = \begin{bmatrix} h(d) & h(d-1) & \cdots & h(d-M+1) \\ h(d+1) & h(d) & \cdots & h(d-M+2) \\ \vdots & \vdots & \ddots & \vdots \\ h(d+v) & h(d+v-1) & \cdots & h(d+v-M+1) \end{bmatrix} \cdot \begin{bmatrix} w(0) \\ w(1) \\ \vdots \\ w(M-1) \end{bmatrix} \equiv H_{win} \cdot w \tag{3-21}$$

and,

$$c_{wall} = \begin{bmatrix} c(0) \\ \vdots \\ c(d-1) \\ c(d+v+1) \\ \vdots \\ c(L+M-2) \end{bmatrix} = \begin{bmatrix} h(0) & 0 & \cdots & 0 \\ \vdots & \vdots & \ddots & \vdots \\ h(d-1) & h(d-2) & \cdots & h(d-M) \\ h(d+v+1) & h(d+v) & \cdots & h(d+v-M+2) \\ \vdots & \vdots & \ddots & \vdots \\ 0 & 0 & \cdots & h(M-1) \end{bmatrix} \cdot \begin{bmatrix} w(0) \\ w(1) \\ \vdots \\ w(M-1) \end{bmatrix} \equiv H_{wall} \cdot w \tag{3-22}$$

The energy inside the window and outside the window can be represented as:

$$c_{win}^T \cdot c_{win} = w^T \cdot H_{win}^T \cdot H_{win} \cdot w = w^T \cdot B \cdot w \tag{3-23}$$

$$c_{wall}^T \cdot c_{wall} = w^T \cdot H_{wall}^T \cdot H_{wall} \cdot w = w^T \cdot A \cdot w \tag{3-24}$$

Our objective is to keep the energy inside the window to be constant and at the same time minimize the energy outside the window by adjusting w. This is equivalent to maximize the SSNR that is defined as:

$$SSNR = \frac{w^T \cdot B \cdot w}{w^T \cdot A \cdot w} \tag{3-25}$$

We assume that B is invertible [11].

The rows of c_{win} are consisted of the shifted windows of the combined channel impulse response. In practical applications, we have found that the rank of the H_{win} is equal to M so that the matrix B can be decomposed by Cholesky Decomposition into:

$$B = Q \cdot \Delta \cdot Q^T = (Q\sqrt{\Delta}) \cdot (\sqrt{\Delta} Q^T) = (Q\sqrt{\Delta}) \cdot (Q\sqrt{\Delta})^T = \sqrt{B} \cdot \sqrt{B}^T \tag{3-26}$$

where Δ is a diagonal matrix with the elements as the eigenvalues of B, and the columns of Q are the orthonormal eigenvectors. Since B is a full rank matrix, the matrix $(\sqrt{B})^{-1}$ existed. We define $y = \sqrt{B}^T \cdot w$ so that,

$$y^T \cdot y = w^T \sqrt{B} \cdot \sqrt{B}^T w = w^T \cdot B \cdot w = 1 \tag{3-27}$$

Using $w = \left(\sqrt{B}^T\right)^{-1} \cdot y$, we could get

$$w^T \cdot A \cdot w = y^T \left(\sqrt{B}\right)^{-1} \cdot A \cdot \left(\sqrt{B}^T\right)^{-1} y = y^T \cdot C \cdot y \tag{3-28}$$

Optimal shortening then can be regarded as choosing y to minimize $y^T Cy$ while satisfying the constraint $y^T \cdot y = 1$. The solution to this problem can be achieved when $y = l_{\min}$ where $l_{\min}$ is the unit-length eigenvector corresponding to the minimum eigenvalues $\lambda_{\min}$ of C. The resulting TEQ coefficients are thus

$$w_{opt} = \left(\sqrt{B}^T\right)^{-1} \cdot l_{\min} \tag{3-29}$$

The optimal shortening SNR can be expressed as

$$SSNR_{opt} = 10\log\left(\frac{w_{opt}^T \cdot B \cdot w_{opt}}{w_{opt}^T \cdot A \cdot w_{opt}}\right) = 10\log\left(\frac{1}{\lambda_{\min}}\right) = -10\log(\lambda_{\min}) \tag{3-30}$$

The solution when B is singular is more complex and the algorithm is given by Melsa, Younce and Rohrs [11].

The MSSNR method minimizes the part of the impulse response that leads to ISI. If we could reduce the energy outside the window to zero, ISI can be totally eliminated and the maximum channel capacity can be achieved.

3.4 Geometric TEQ Method

Geometric TEQ Method is the first method to optimize the equalizer for maximum bit rate [12]. With this method, we first design a TIR to maximize the bit rate on one of the

DMT sub-channels. Then the equalizer is calculated using MMSE method and the above TIR.

We assume that the sub-channel could be modeled as additive white Gaussian noise (AWGN) channels,

$$b_{DMT} = \sum_{i=1}^{N} \log_2\left(1+\frac{SNR_i}{\Gamma_i}\right) \tag{3-31}$$

where i is the sub-channel index, SNR_i is the signal noise ratio and Γ_i is the SNR gap of the i^{th} sub-channel. Assuming that the SNR gap is constant in all the sub-channel so that $\Gamma_i = \Gamma \forall i$. We define a average SNR, $\overline{SNR}$, by

$$1+\frac{\overline{SNR}}{\Gamma} = \left[\prod_{i=1}^{N}\left(1+\frac{SNR_i}{\Gamma}\right)\right]^{1/N} \tag{3-32}$$

or

$$\overline{SNR} = \Gamma \cdot \left\{\left[\prod_{i=1}^{N}\left(1+\frac{SNR_i}{\Gamma}\right)\right]^{1/N} - 1\right\} \tag{3-33}$$

we could get

$$b_{DMT} = N \cdot \log_2\left(1+\frac{\overline{SNR}}{\Gamma}\right) \tag{3-34}$$

If the input SNR is high enough, we could simplify the expression of $\overline{SNR}$ as

$$\overline{SNR} = \left[\prod_{i=1}^{N}(SNR_i)\right]^{1/N} \tag{3-35}$$

From the above equations, we could find that maximize SNR_i will maximize $\overline{SNR}$ so that the channel capacity b_{DMT} is maximized. This is the key point in geometric TEQ design.

Without considering ISI, the SNR_i can be expressed as

$$SNR_i = \frac{S_{xx} \cdot |T_i|^2}{S_{nn,i} \cdot |W_i|^2} \tag{3-36}$$

where S_{xx} is the signal power, $S_{nn,i}$ is the noise power in the i^{th} sub-channel and T_i, W_i are respectively the amplitude gain of the TIR t and the TEQ w.

Define

$$L(b) = \frac{1}{N} \cdot \sum_{i=1}^{N} \ln|T_i|^2 \tag{3-37}$$

The problem to maximize the average SNR, $\overline{SNR}$, is converted to maximize the L(b). This optimization problem does not have a closed-form solution but it may be solved by numerical method.

3.5 Summary

Three TEQ design methods are discussed. MMSE method is more classical and simple to understand. MSSNR method is more direct. Geometric Method cannot guarantee the convergence of the solution.

Chapter 4

Proposed TEQ Design Methods

In the previous chapter, we discussed three TEQ design methods. We noticed that the MSSNR method was a sub-optimal method that maximizes the channel capacity and the solution is guaranteed. But it still cannot totally eliminate the ISI since we cannot find a solution that forces the energy outside the window to be zero. In this chapter, we first propose a modified method based on MMSE method and then propose a new method that could theoretically totally eliminate the ISI.

4.1 Modified MMSE Method

MMSE method was discussed in chapter 3; it is the most popular TEQ design method in DMT system.

From Equation 3-3 and 3-4, we found that the MMSE method tries to minimize the mean square error between the target impulse response and the effective impulse response.

$$MSE = E\left(\left(t^T \cdot x_k - w^T \cdot y_k\right)\cdot\left(t^T \cdot x_k - w^T \cdot y_k\right)^*\right) \qquad (4\text{-}1)$$

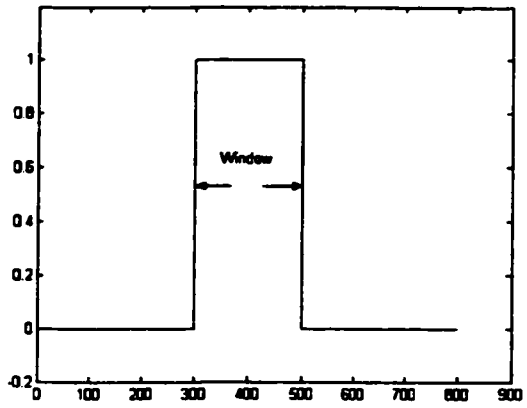

Figure 4.1 Target Impulse Responses

Suppose the target impulse response takes a rectangular shape (Figure 4.1). The MMSE design method attempts to make the effective channel impulse response approach the shape of the target impulse response. The difference between the target impulse response and the effective impulse response is measured by MSE in Equation 4-1. The MMSE method tries to concentrate the energy of the effective impulse response into the rectangular window of the target impulse response and at the same time distribute the MSE equally along the effective impulse response, as Figure 4-2 shows.

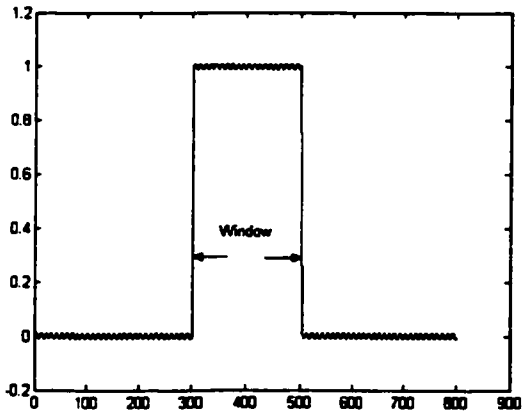

Figure 4.2 MSE Distributions

Very large MSE means that the TEQ does not have enough power to concentrate the effective impulse response energy and very small MSE means the TEQ could distribute

the error equally. Considering about the aim to put as much energy as possible into the TIR window in TEQ design, we find that both very small MSE and very large MSE are not the best choice. In either circumstance, TEQ puts more energy outside the window and introduce more ISI.

The length of the MMSE TEQ is directly related to its power to concentrate the energy and distribute the mean square error. If the TEQ length is too short, it does not have enough power to concentrate the effective impulse response energy, if the TEQ length is too long, it has enough power to distribute the MSE equally. We could conclude that the performance of the MMSE TEQ will increase as its length increases when the length is very small. After the TEQ achieves its best performance with some certain length, continuing to increase its length will degrade its performance.

From the above discussions, we find out that minimum MSE does not guarantee the best performance. To solve the problem, we modify the MMSE method a little. Rewrite Equation 3-14 here as Equation 4-2,

$$t = \frac{R_{\Delta}^{-1} \cdot e_i}{R_{\Delta}^{-1}(i,i)} \tag{4-2}$$

we do not choose the t correspond to $i_{opt} = \arg\max_{0 \le i \le v} \{R_{\Delta}^{-1}(i,i)\}$ but rather calculate all the possible w by

$$t^T \cdot R_{xy} = w^T \cdot R_{yy} \tag{4-3}$$

Then we choose the w that leads to maximum SSNR given by the Equation 4-4.

$$SSNR = \frac{w^T \cdot B \cdot w}{w^T \cdot A \cdot w} \tag{4-4}$$

where B and A are defined in 3-23 and 3-24 respectively.

Instead of using MSE, we use SSNR as the design criterion in modified MMSE method. In equation 4-3, we do not choose the t that leads to the minimum MSE but t that leads to maximize SSNR. Simulation results show that Modified MMSE method generates a more effective TEQ than the MMSE method does.

4.2 Multirate Time Domain Equalizer Design

We assume the length of the impulse response of the physical channel h is L, the length of the TEQ w is M and the length of the TIR t is T. Using convolution theory, we know that the length of the effective channel impulse response y is $L+M-1$. In order to perfectly eliminate the ISI, all the energy outside the TIR window should be forced to zero. The relationship between the effective channel impulse response, physical channel impulse response and the TEQ can be described as,

$$\begin{bmatrix} y_0 \\ y_1 \\ y_2 \\ \vdots \\ \vdots \\ \vdots \\ y_{L+M-4} \\ y_{L+M-3} \\ y_{L+M-2} \end{bmatrix} = \begin{bmatrix} h(0) & 0 & \cdots & \cdots & \cdots & \cdots & 0 \\ h(1) & h(0) & 0 & \cdots & \cdots & \cdots & 0 \\ h(2) & h(1) & h(0) & 0 & \cdots & \cdots & 0 \\ \vdots & \ddots & \ddots & \ddots & \ddots & \ddots & \vdots \\ h(M-1) & \cdots & \cdots & \cdots & \cdots & \cdots & h(0) \\ \vdots & \ddots & \ddots & \ddots & \ddots & \ddots & \ddots \\ 0 & \cdots & \cdots & 0 & h(L-1) & h(L-2) & h(L-3) \\ 0 & \cdots & \cdots & \cdots & 0 & h(L-1) & h(L-2) \\ 0 & \cdots & \cdots & \cdots & \cdots & 0 & h(L-1) \end{bmatrix} \cdot \begin{bmatrix} w_0 \\ w_1 \\ w_2 \\ \vdots \\ \vdots \\ \vdots \\ w_{M-3} \\ w_{M-2} \\ w_{M-1} \end{bmatrix} \tag{4-5}$$

Let Y represent the effective channel impulse response vector, H represent the physical channel convolution matrix and W represent the TEQ, the equation can be rewritten as,

$$Y = H \cdot W \tag{4-6}$$

From the above equations, we found that in order to eliminate ISI, we should let T+1 taps of Y open and set all the other L+M-T-2 taps to be zero. Let Y' be $[0 \ \cdots \ \cdots \ 0 \ X \ 0 \ \cdots \ \cdots \ 0]$, where X is a $(T+1)\times 1$ matrix with arbitrary value, we get Equation 4-7:

$$\begin{bmatrix} y_0 \\ y_1 \\ y_2 \\ \vdots \\ \vdots \\ \vdots \\ y_{L+M-4} \\ y_{L+M-3} \\ y_{L+M-2} \end{bmatrix} = \begin{bmatrix} h(0) & 0 & \cdots & \cdots & \cdots & \cdots & 0 \\ h(1) & h(0) & 0 & \cdots & \cdots & \cdots & 0 \\ h(2) & h(1) & h(0) & 0 & \cdots & \cdots & 0 \\ \vdots & \ddots & \ddots & \ddots & \ddots & \ddots & \vdots \\ h(M-1) & \cdots & \cdots & \cdots & \cdots & \cdots & h(0) \\ \vdots & \ddots & \ddots & \ddots & \ddots & \ddots & \ddots \\ 0 & \cdots & \cdots & 0 & h(L-1) & h(L-2) & h(L-3) \\ 0 & \cdots & \cdots & \cdots & 0 & h(L-1) & h(L-2) \\ 0 & \cdots & \cdots & \cdots & \cdots & 0 & h(L-1) \end{bmatrix} \cdot \begin{bmatrix} w_0 \\ w_1 \\ w_2 \\ \vdots \\ \vdots \\ \vdots \\ w_{M-3} \\ w_{M-2} \\ w_{M-1} \end{bmatrix} = \begin{bmatrix} 0 \\ \vdots \\ 0 \\ \times \\ \vdots \\ \times \\ 0 \\ \vdots \\ 0 \end{bmatrix} \tag{4-7}$$

Representing equation 4-7 as equation 4-8

$$Y' = H \cdot W \tag{4-8}$$

then W could be attained using Gaussian elimination:

$$W = H \setminus Y' \tag{4-9}$$

We note that the number of the unknown variables is M and the number of the equations is L+M-T-2. In order to guarantee that the solution exists, the number of the unknown variables should be greater than or equal to the number of the equations. So

$$L + M - T - 2 \le M \tag{4-10}$$

we get

$$T \ge L - 2 \tag{4-11}$$

Equation 4-11 shows that in order to totally eliminate the ISI, the length of the target channel impulse response T must be greater than or equal to L-2 which means that the impulse response can only be shortened by 2 and we must use a cyclic prefix as long as L-3. Obviously this cannot satisfy our requirement.

Ungerboeck proposed a zero ISI FIR with better spectral concentration [14]. Based on Ungerboeck' work, we propose a Multirate TEQ design method which could guarantee Zero ISI in the sampling point. The revised system diagram is given in Figure 4.3.

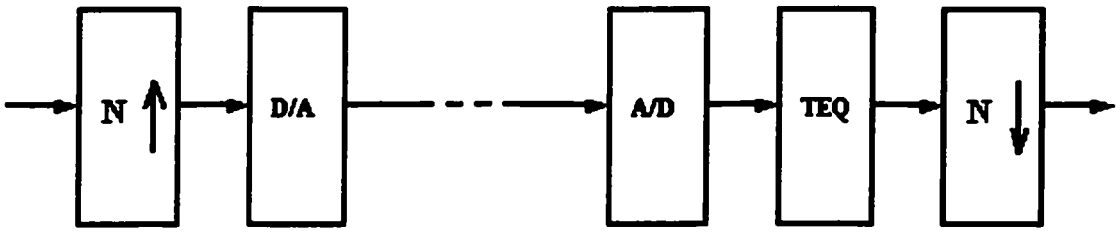

Figure 4.3 Revised System Diagram

Using multi-rate technique, the previous method could be improved and become practical. We interpolate the transmitted signal by N before the signal is fed into the A/D converter. In the receiver side, decimation by N is performed after the received signal passed the TEQ. Obviously the TEQ operates at a higher sampling rate in this method. This can be represented as,

$$H(z) \cdot W(z)\big|_{\downarrow N} = z^{-L_c} + z^{-L_c+1} \cdots z^{-L_c+T} \qquad (4\text{-}12)$$

where L_c is the delay of the equalized impulse response.

After adopting the interpolator with interpolate parameter N, the length of the physical channel becomes $N \cdot L$ and the length of the TIR becomes $N \cdot T$. The length of the TEQ does not change but TEQ will work at a higher frequency.

In multi-rate TEQ method, we get Equation 4-13 after interpolation:

$$\begin{bmatrix} y_0 \\ y_1 \\ y_2 \\ \vdots \\ \vdots \\ \vdots \\ y_{N\cdot L+M-4} \\ y_{N\cdot L+M-3} \\ y_{N\cdot L+M-2} \end{bmatrix} = \begin{bmatrix} h(0) & 0 & \cdots & \cdots & \cdots & \cdots & 0 \\ h(1) & h(0) & 0 & \cdots & \cdots & \cdots & 0 \\ h(2) & h(1) & h(0) & 0 & \cdots & \cdots & 0 \\ \vdots & \ddots & \ddots & \ddots & \ddots & \ddots & \vdots \\ 0 & \cdots & h(N\cdot L-1) & \cdots & h(0) & \cdots & 0 \\ \vdots & \ddots & \ddots & \ddots & \ddots & \ddots & \ddots \\ 0 & \cdots & \cdots & 0 & h(N\cdot L-1) & h(N\cdot L-2) & h(N\cdot L-3) \\ 0 & \cdots & \cdots & \cdots & 0 & h(N\cdot L-1) & h(N\cdot L-2) \\ 0 & \cdots & \cdots & \cdots & \cdots & 0 & h(N\cdot L-1) \end{bmatrix} \cdot \begin{bmatrix} w_0 \\ w_1 \\ w_2 \\ \vdots \\ \vdots \\ \vdots \\ w_{M-3} \\ w_{M-2} \\ w_{M-1} \end{bmatrix} = \begin{bmatrix} 0 \\ \vdots \\ 0 \\ \times \\ \vdots \\ \times \\ 0 \\ \vdots \\ 0 \end{bmatrix}$$

(4-13)

The number of the unknown variable is still M and the number of the equations becomes $N \cdot L + M - 1$, among which $N \cdot (T+1)$ equations are left open and the other $N \cdot (L-1) + M - 1 - N \cdot T$ equations should be set to zero.

In the receiver side, we keep one equation in every N equations after decimation. The equations left are shown in Equation 4-14. The number of the unknown variables is still M but the number of equations becomes $(N \cdot L + M - 1)/N$ in which T+1 equations can be left open.

$$\begin{bmatrix} y_0 \\ y_N \\ y_{2N} \\ \vdots \\ \vdots \\ \vdots \\ \vdots \\ \vdots \\ y_{N\cdot L+M-2} \end{bmatrix} = \begin{bmatrix} h(0) & 0 & \cdots & \cdots & \cdots & \cdots & 0 \\ h(N) & h(N-1) & \cdots & h(0) & 0 & \cdots & 0 \\ h(2N) & \cdots & \cdots & \cdots & h(0) & \cdots & 0 \\ \vdots & \ddots & \ddots & \ddots & \ddots & \ddots & \vdots \\ 0 & \cdots & \cdots & \cdots & h(0) & \cdots & 0 \\ \vdots & \ddots & \ddots & \ddots & \ddots & \ddots & \ddots \\ 0 & \cdots & \cdots & \cdots & \cdots & \cdots & h(N\cdot L-2N) \\ 0 & \cdots & \cdots & \cdots & \cdots & \cdots & h(N\cdot L-N) \\ 0 & \cdots & \cdots & \cdots & \cdots & 0 & h(N\cdot L-1) \end{bmatrix} \cdot \begin{bmatrix} w_0 \\ w_1 \\ w_2 \\ \vdots \\ \vdots \\ \vdots \\ w_{M-3} \\ w_{M-2} \\ w_{M-1} \end{bmatrix} = \begin{bmatrix} 0 \\ \vdots \\ 0 \\ \times \\ \vdots \\ \times \\ 0 \\ \vdots \\ 0 \end{bmatrix}$$

(4-14)

To guarantee that a solution exists, Equation 4-15 should be satisfied,

$$(N \cdot L + M - 1)/N - (T + 1) \leq M \tag{4-15}$$

Solve this equation, we get

$$M \geq \frac{N}{N-1} \cdot (L - T - 1) - 1 \tag{4-16}$$

Equation 4-16 shows that we could solve the problem numerically with multirate method and a solution is guaranteed without the restriction that T must be greater than or equal to L-2. This is important because we could choose T arbitrarily, which means we have control on the length of the impulse response of the effective channel.

For a special case, L and T are determined. M approaches L-T-2 when N increases to infinity which means the minimum number of the TEQ taps is L-T-2. If we choose N equal to 2 then the number of the TEQ taps is 2*(L-T)-3. With such a TEQ we could shorten the channel impulse response perfectly into T samples.

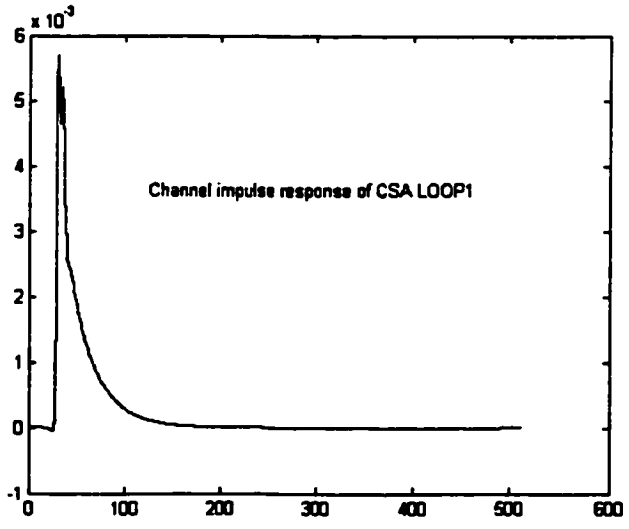

Figure 4.4 Channel Impulse Response of CSALoop1

Figure 4.4 is the channel response of the CSA Loop1. Using multirate method, we could shorten the channel response arbitrarily.

Set T = 32 and N = 2, we get a truncated TEQ in Figure 4.5:

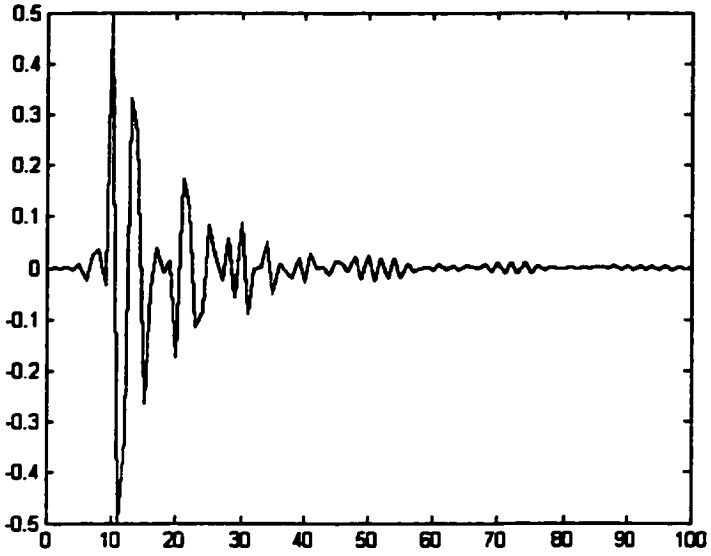

Figure 4.5 Multirate TEQ

The equalized channel impulse response is shown in Figure 4.6,

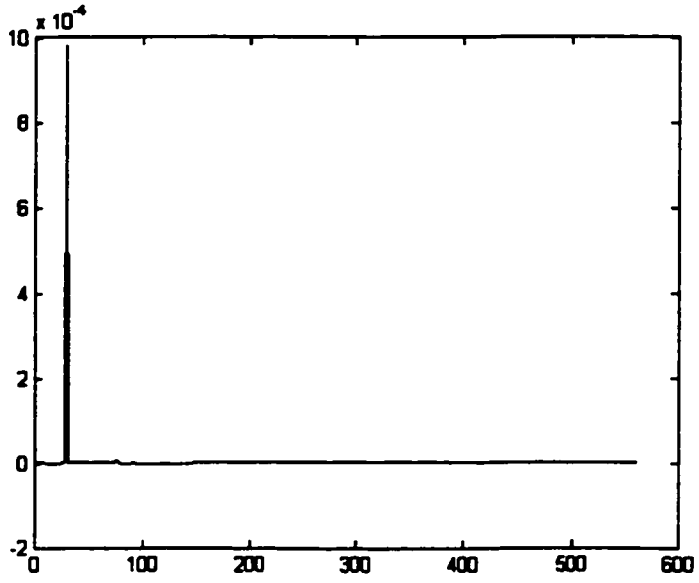

Figure 4.6 Shortened Channel Impulse Response

4.3 Multirate Zero ISI (MRZISI) TEQ Design

In the previous section, a multirate time domain equalizer design method is proposed. It enables us to design the TEQ numerically and have more control on the result. Based on this method, we could easily design a zero ISI time domain equalizer. With Zero ISI TEQ, it is possible for us to discard the cyclic prefix, which increases the data transmission rate and decreases the system complexity.

We have proved that we could shorten the length of the channel impulse response into T samples. In order to achieve Zero_ISI, we just set T equal to 1 and the Equation 4-12 becomes Equation 4-17,

$$H(z) \cdot W(z)\big|_{\downarrow N} = z^{-L_c} \tag{4-17}$$

We could put 1 at arbitrary place that leads to different channel response delays (L_c). With different channel delays and interpolation factors, we could get more solutions and the best solution is chosen based on the criterion presented in the previous chapter.

$$\begin{bmatrix} y_0 \\ y_N \\ y_{2N} \\ \vdots \\ \vdots \\ \vdots \\ \vdots \\ \vdots \\ y_{N\cdot L+M-2} \end{bmatrix} = \begin{bmatrix} h(0) & 0 & \cdots & \cdots & \cdots & \cdots & 0 \\ h(N) & h(N-1) & \cdots & h(0) & 0 & \cdots & 0 \\ h(2N) & \cdots & \cdots & \cdots & h(0) & \cdots & 0 \\ \vdots & \ddots & \ddots & \ddots & \ddots & \ddots & \vdots \\ 0 & \cdots & \cdots & \cdots & h(0) & \cdots & 0 \\ \vdots & \ddots & \ddots & \ddots & \ddots & \ddots & \ddots \\ 0 & \cdots & \cdots & \cdots & \cdots & \cdots & h(N\cdot L-2N) \\ 0 & \cdots & \cdots & \cdots & \cdots & \cdots & h(N\cdot L-N) \\ 0 & \cdots & \cdots & \cdots & \cdots & 0 & h(N\cdot L-1) \end{bmatrix} \cdot \begin{bmatrix} w_0 \\ w_1 \\ w_2 \\ \vdots \\ \vdots \\ \vdots \\ w_{M-3} \\ w_{M-2} \\ w_{M-1} \end{bmatrix} = \begin{bmatrix} 0 \\ \vdots \\ 0 \\ 1 \\ 0 \\ \vdots \\ 0 \\ \vdots \\ 0 \end{bmatrix} \tag{4-18}$$

If we set N=2 and T=1 in Equation 4-16, we get

$$M \geq \frac{N}{N-1} \cdot (L-1) - 1 = \frac{2}{2-1} \cdot (L-1) - 1 = 2L - 3 \qquad (4\text{-}19)$$

This shows us that we could achieve Zero_ISI using a TEQ with $2L$-3 taps, where L is the length of the physical channel. If we increase N, the number of the TEQ taps will approach L-2.

The typical length of the channel impulse response L is about 512 samples under the sampling rate of 2.024 MHz. According to Equation 4-16, we need a really long TEQ with at least 510 taps to achieve zero ISI. However we find that most of the designed TEQ taps in simulation are almost zero and could be discarded. In this way, we could shorten the TEQ by 90% without degrading its performance significantly.

4.4 Discussion of Noise Effect

So far no other restrictions on the filters (other than the zero ISI condition) have been applied. It is desirable to maximize signal-to-noise ratio by using matched transmitter and receiver filters [42]. However, their design is more complicated as it involves the solution of simultaneous non-linear (quadratic) equations. This is because the receiver filter coefficients are the same as the transmitter filter coefficients, but in time reversed order. This makes it harder to find the zero ISI filters, because simultaneous quadratic equations need to be solved.

Recall the condition for no intersymbol interference:

$$H(z) \cdot W(z)\big|_{\downarrow N} = z^{-L_c} \qquad (4\text{-}20)$$

This can be satisfied exactly only when the channel is known precisely. Otherwise, there will be some residue. In other words, let $\delta \cdot H(z)$ be the error in the channel taps, then ISI results become

$$\delta \cdot H(z) \cdot W(z)\big|_{\downarrow N} \neq 0 \tag{4-21}$$

Thus, the sensitivity of the filter coefficients to fluctuations in the channel is governed by the channel taps. Thus, instead of the multirate zero ISI condition one obtains

$$W(z) \cdot \left[H(z) + \delta \cdot H(z)\right]_{\downarrow N} = z^{-L_c} + \Delta(z) \tag{4-22}$$

If the correct filter is $W(z) + \delta \cdot W(z)$ so that

$$\left[H(z) + \delta \cdot H(z)\right] \cdot \left[W(z) + \delta \cdot W(z)\right]_{\downarrow N} = z^{-L_c} \tag{4-23}$$

then

$$-\Delta(z) = \delta \cdot W(z) \cdot \left[H(z) + \delta \cdot H(z)\right]_{\downarrow N} \tag{4-24}$$

Thus, instead of z^{-L_c} one gets $z^{-L_c} + \Delta z$ so that the error due to inaccurate determination of channel is Δz. Note that Δz is large if $\delta \cdot W(z)$ is large, it is desirable that $W(z)$ taps be as small as possible so that the fractional change is small.

Apart from noise in the channel taps, there is also the additive noise due to the channel. If the noise is Δz_{noise}, the zero ISI condition is modified to

$$\left(H(z) \cdot W(z) + \Delta z_{noise}\right)_{\downarrow N} = z^{-L_c} \tag{4-25}$$

A good choice of $W(z)$ could be determined as follows: determine the product $H(z) \cdot W_i(z)$ where $W_i(z)$ is the zero ISI filter corresponding to the choice of delay z^{-i} and form a vector from the filter coefficients in the product. In other words, perform a convolution of the channel with each of the candidate zero ISI filters. Ideally, this

convolution should just be a delay, but that cannot be the case in general. Then the filter whose convolution with the channel has the least norm is selected. Clearly, this is not rigorous method of choosing the best filter from the set, but a simple and practical one.

4.5 Complexity Comparison of the TEQ Design Methods

Computation complexity is an important factor to be considered when we choose design method. Computation complexity partially determines the hardware complexity. In our discussion, we only consider the high complexity operations such as inverse of the matrix, Cholesky decomposition of matrix and matrix multiplex.

Table 4-1 gives the detail computational complexity of MMSE method; some notations used in the table are illustrated as following:

Ls: Length of the signal
L: Length of the channel
Nt: Length of the target impulse response
Ne: Length of the time domain equalizer
N: Interpolation factor

Description	Multiply	Add
Compute Rxx, Rxy and Ryy	Nt*Ls+Ne*Ls*2	Nt*Ls+Ne*Ls*2
Inv(Ryy)	$(5Ne^3+Ne)/3$	$(5Ne^3+Ne)/3$
Rxy*inv(Ryy)*Rxy'	$Ne^2*Nt+Nt^2*Ne$	$Ne^2*Nt+Nt^2*Ne$
Inv(Rd)	$(5Nt^3+Nt)/3$	$(5Nt^3+Nt)/3$
Inv(Ryy)*Rxy'*TIR	$Ne^2*Nt+Nt*Ne$	$Ne^2*Nt+Nt*Ne$

Table 4-1 MMSE Computational Complexity

Table 4-2 gives the computational complexity of MSSNR method:

Description	Multiply	Add
Compute A	(L-Nt)*Ne	(L-Nt)*Ne
Compute B	Nt*Ne+(Ne+1)*Ne/2	Nt*Ne+(Ne+1)*Ne/2
Cholesky decomposition of B	Ne^3	Ne^3
Calculate $\left(\sqrt{B}\right)^{-1}$	$(5*Ne^3+Ne)/3$	$(5*Ne^3+Ne)/3$
Calculate C	$2*Ne^3$	$2*Ne^2*(Ne-1)$
Calculate C^{-1}	$(5*Ne^3+Ne)/3$	$(5*Ne^3+Ne)/3$
Calculate w_{opt}	Ne^2	(Ne-1)*Ne

Table 4-2 MSSNR Computational Complexity [53]

MRZISI method is shown in Table 4-3, where we set N=2:

Description	Multiply	Add
Gaussian elimination of matrix H in equation 5-10	$4*L^2$	$4*L^2$

Table 4-3 MRZISI Computational Complexity

In our simulation, we use Ls=1000, L=512 and Nt=32. Ne depends on the method we use, Ne equals 12 in MMSE method, equals 32 in MSNNR method and equals 64 in MRZISI method. Based on these parameters, we get the number of multiplication and addition needed for each method:

	Multiplication	Addition
MMSE	147300	147300
MSSNR	225488	223440
MRZISI	1048576	1048576

Table 4-4 Comparison of Computational Complexity

From Table 4-4, we find that the number of multiplication operation of MRZISI method is about seven times of MMSE method and about four times of MSSNR method. The number of addition operation of MRZISI method is also about seven times of MMSE method and about four times of MSSNR method.

Hardware complexity is also considered. TEQ designed with MRZISI method works at the speed twice of the speed of the TEQ designed by other design methods. This requires higher speed ADC and DAC which in my opinion is acceptable. But the frequency response of the equalized channel got from MRZISI method is perfectly linear so that we do not need another equalizer which may be adopted in other methods to deal with the phase distortion.

We also concern with the length of the TEQ and the delay introduced by the TEQ, these problems are addressed in chapter 5 based on our simulation result.

4.6 Additional Remarks

The following remarks clarify some aspects of the proposed multirate system.

- The zero ISI filters clearly depend on the channel and interpolation rate N. This is obvious from the above analysis.

- There is no solution for finite number of filter coefficients when N=1. The infinite-tap solution is given by $H(z) \cdot W(z) = 1$, so that $W(z) = 1/H(z)$. This is the well known zero forcing equalizer.

- Contrast with the case of linear equalizer with the peak distortion criterion. The complete elimination of the ISI requires the use of an inverse filter for $H(z)$. Such an equalizer requires an infinite number of taps when implemented by a FIR filter. Any FIR filter with a finite number of taps will always have ISI. In our discussion above, ISI has been eliminated with a FIR filter with a finite number of taps. The

key is to use multirate signal processing, which involves fewer equations and is solvable using a finite number of taps. The minimum length of TEQ is determined by interpolation factor, as discussed in the previous section.

- The multirate theory gives us a general way of designing zero ISI filters. As noted above, N has to be greater than 1. The larger the value of N, the fewer the conditions to be satisfied and the shorter is the length of the zero ISI filter. Thus, for a given length the interpolation factor gives us greater freedom in design of a zero ISI filter. This additional degree of freedom can be used to design filters with additional desirable properties.

- The relevant matrix has been assumed to be nonsingular. In fact, most of convolution matrix generated by the real channel is nonsingular.

- MRZISI method leads to a totally none ISI effective channel which can be used in DSL system and also be used in other communication systems.

Chapter 5

Simulation Results

Simulation is conducted in MatLab. The results and analysis are presented in this chapter. The downlink of DSL transceiver is used in the simulation. The IFFT and FFT lengths are 512 and a cyclic prefix of 32 is assumed. The signal power at the transmitter output is set to 14 dBm and an additive white Gaussian noise (AWGN) with –140 dBm/Hz power is employed. FEXT is generated according to Equation 2-4. The sampling rate is 2.208 MHz. In the simulation, it is assumed that the accurate channel information is available. Simulation results without precise channel information are given in section 5.5. The channel models used in the simulation are base on Gauge 26 wire.

5.1 Simulation Results of MMSE Method

As discussed in section 4.1, the length of the MMSE TEQ directly determined the TEQ performance. In order to achieve the best TEQ performance, we first attempt to determine how many taps we should use when we design TEQ with MMSE method. We test the performance of MMSE TEQ with different length in our simulation and the results are given in Figure 5.1. We notice that in order to achieve the best performance, the MMSE TEQ length should be between 4 to 20 taps. We choose 16 taps in our simulation.

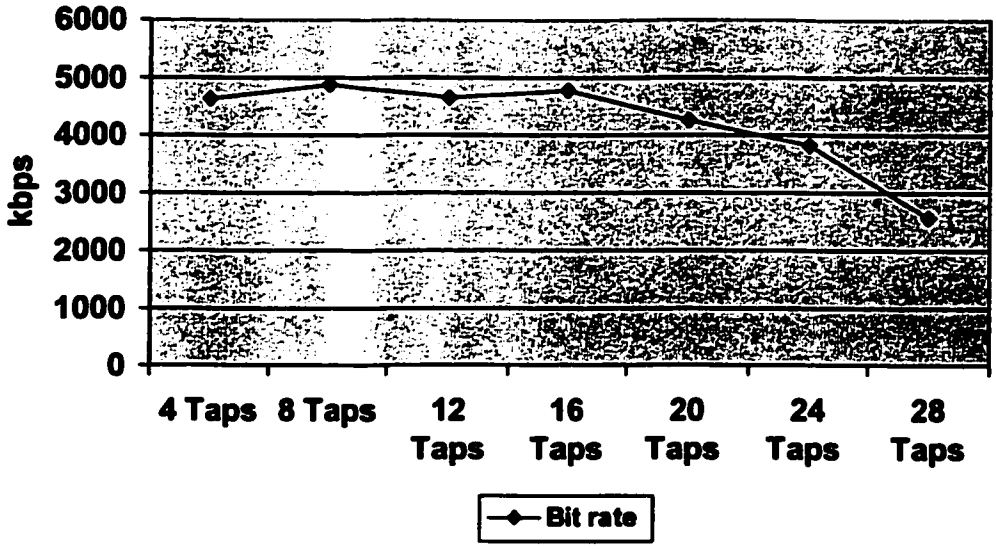

Figure 5.1 Achieved Bit Rate of MMSE TEQ with Different Length

The channel response of CSALoop 2 is shown in Figure 5.2. We note that impulse response of CSALoop2 has a very long tail which leads to severe intersymbol interference.

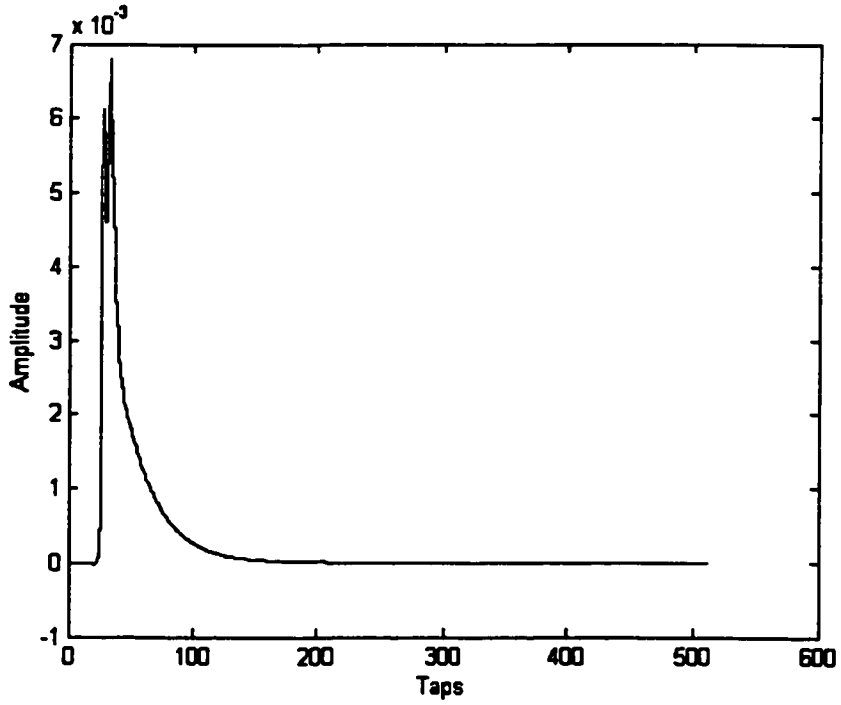

Figure 5.2 Channel Impulse Response of CSALoop 2

Using MMSE TEQ design method, we get a TEQ with 16 taps:

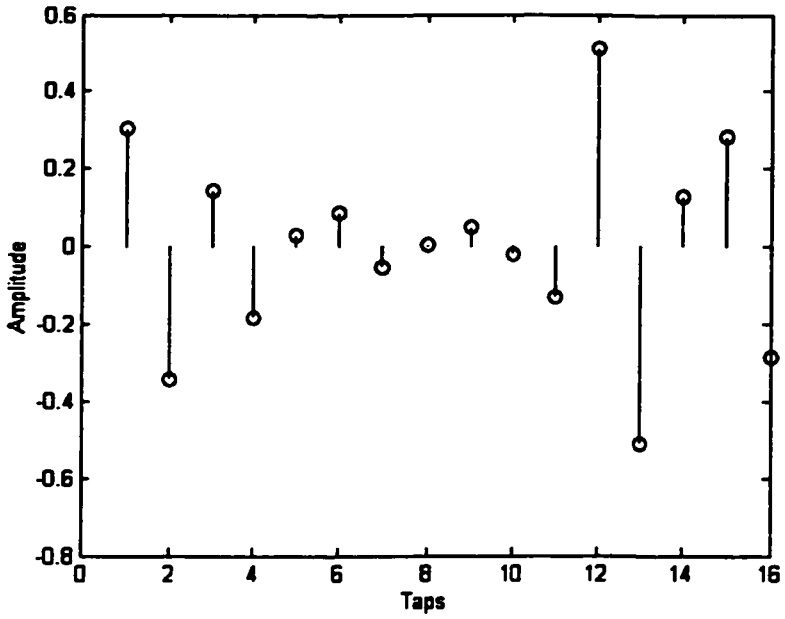

Figure 5.3 TEQ Taps Designed with MMSE Method

The impulse response of the shortened CSALoop2 channel is given in the Figure 5.4:

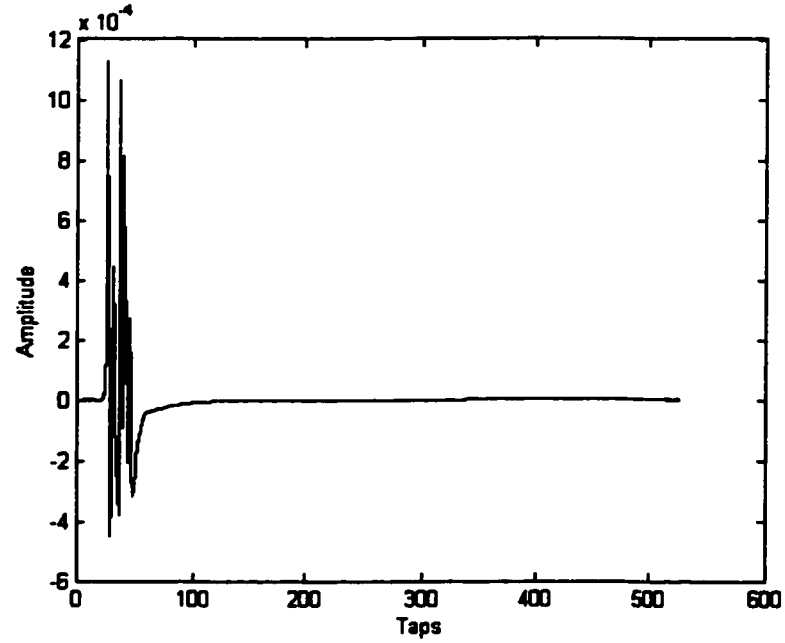

Figure 5.4 Shortened Channel Impulse Response with MMSE Method

We observe from Figure 5.4 that the shortened channel impulse response is more concentrated but there is still a small tail that introduces ISI and worsen the system performance. The frequency response of the shortened channel is shown in Figure 5.5.

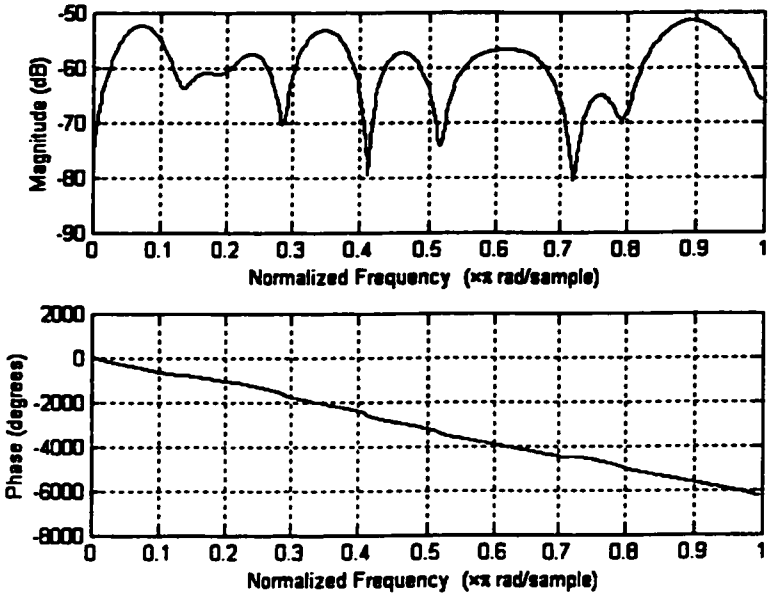

Figure 5.5 Shortened Channel Frequency Response with MMSE Method

Figure 5.6 gives the impulse response of CSALoop7:

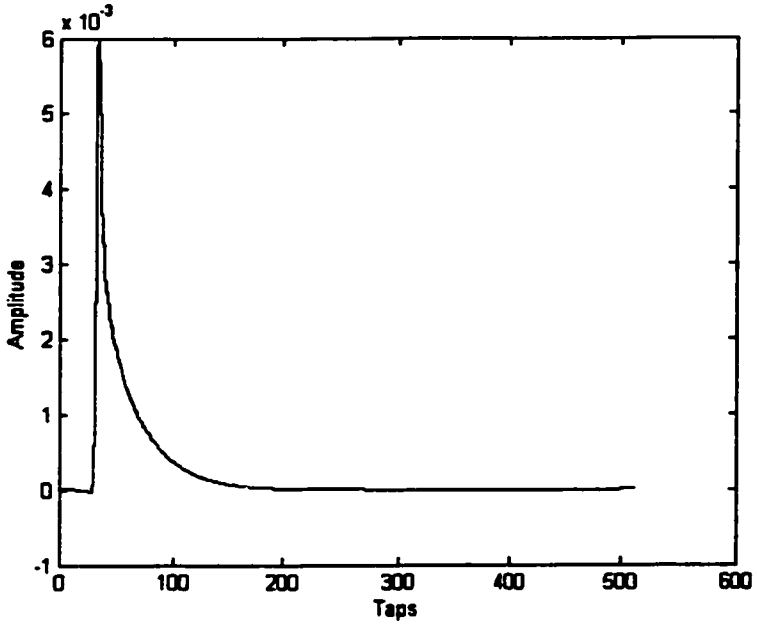

Figure 5.6 Channel Impulse Response of CSALoop 7

Using MMSE method, we get another TEQ with 16 taps:

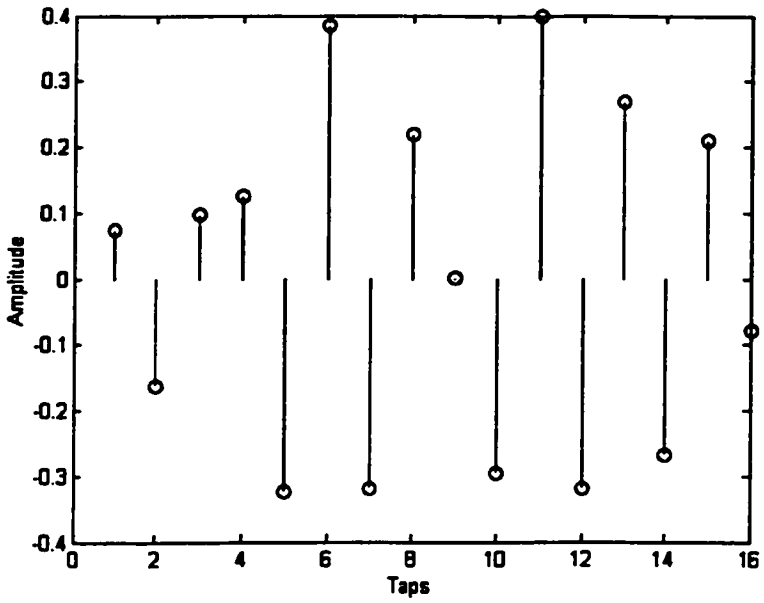

Figure 5.7 TEQ Designed with MMSE Method

The impulse response of the CSALoop7 shortened channel is given in Figure 5.8:

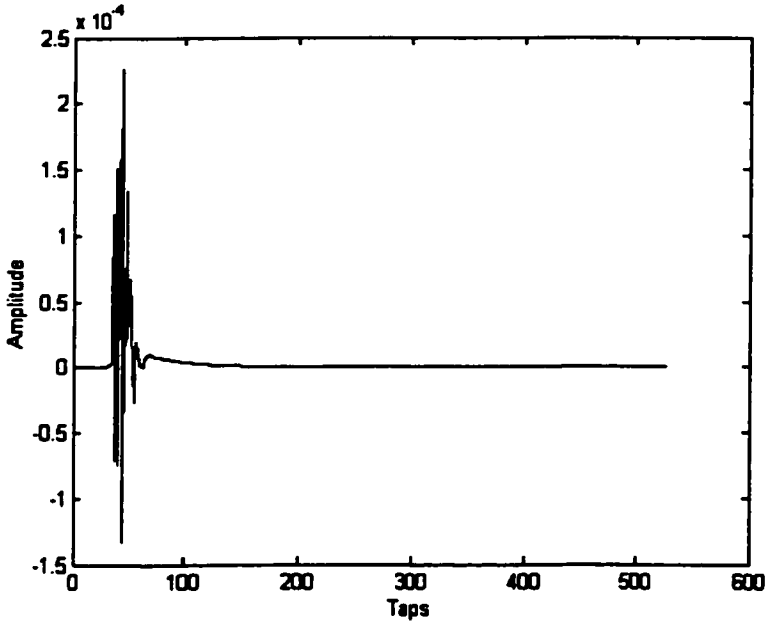

Figure 5.8 Shortened Channel with MMSE Method

We also noticed a little tail in the shortened channel impulse response that degrades the TEQ performance. The frequency response is shown in Figure 5.9:

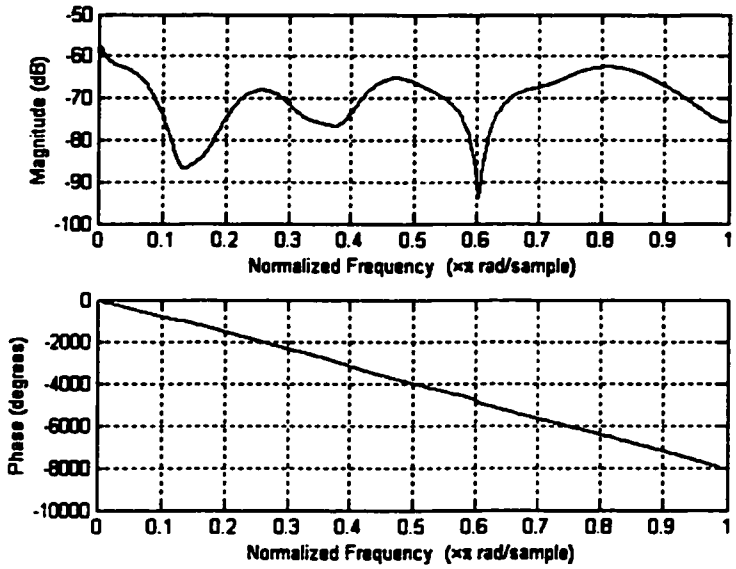

Figure 5.9 Shortened Channel Frequency Response with MMSE Method

Using TEQ designed with MMSE method, the achieved bit rates on different CSA loops are shown in Figure 5.10.

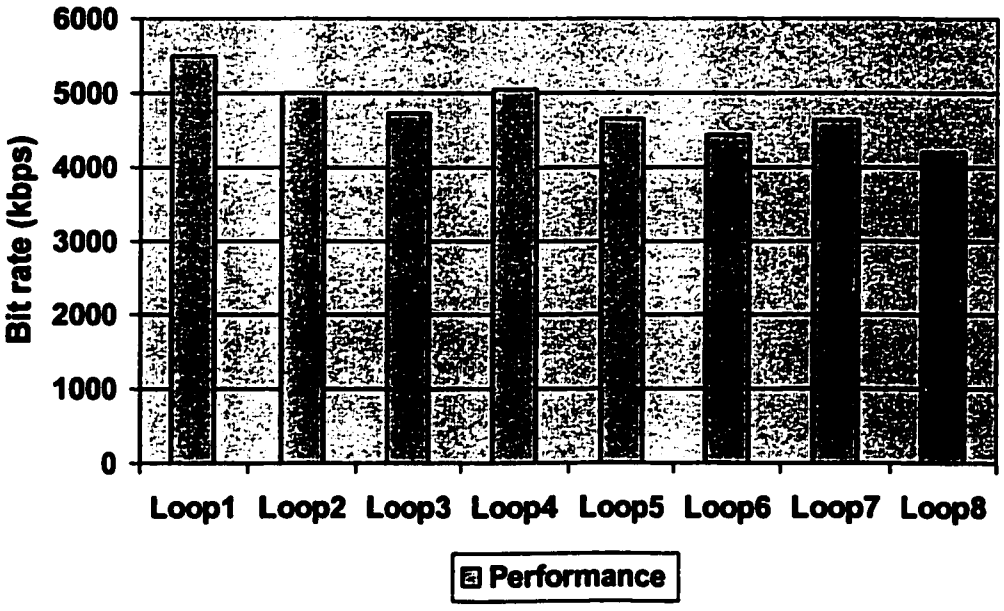

Figure 5.10 Achieved Bit Rate of MMSE Method

The average bit rate is about 1200 bit per symbol (in this chapter, symbol means a DMT transmission block) and equal to about 4.8Mbit per second which is an acceptable performance.

5.2 Simulation Results of Modified MMSE Method

Since MSE is not a good criterion in TEQ design as discussed in section 4.1, The criterion used in MMSE design method is changed. We employ SSNR instead of MSE as the criterion in our new method, which is called modified MMSE method.

Figure 5.11 shows the TEQ designed for CSA Loop3 using modified MMSE method with length equal to 16.

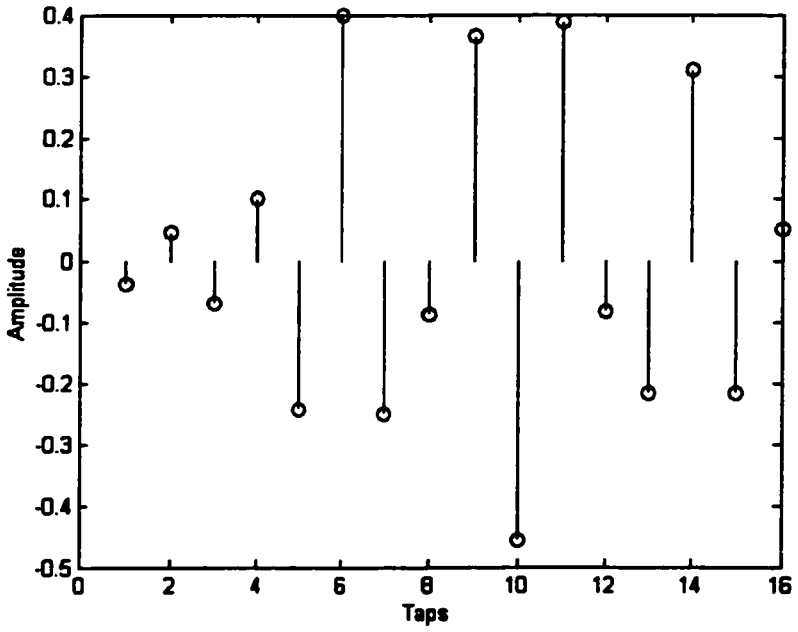

Figure 5.11 TEQ Designed by Modified MMSE Method

The impulse response of the shortened channel is demonstrated in Figure 5.12.

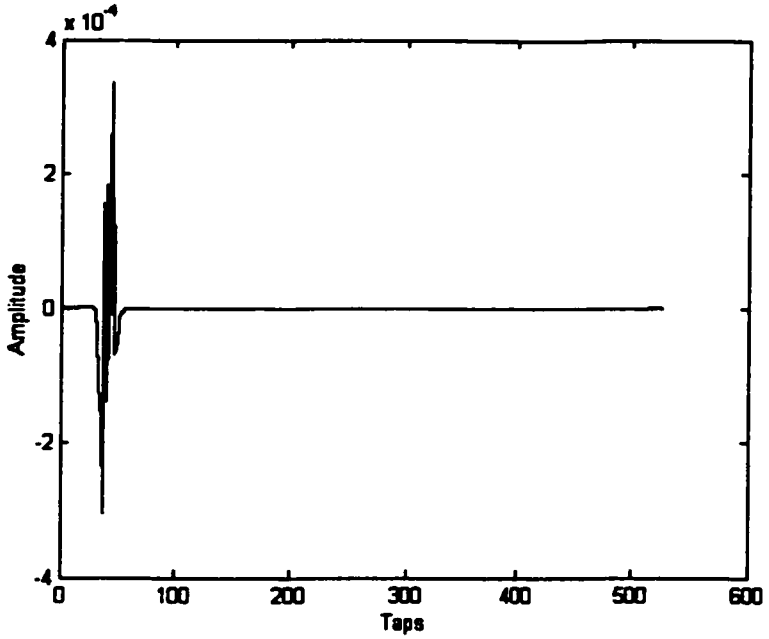

Figure 5.12 Shortened Impulse Response

Compared to the TEQ designed by MMSE method, the tail of the shortened impulse response is smaller which results in a smaller ISI residue and a much better TEQ performance. The frequency response of the shortened channel is shown in Figure 5.13:

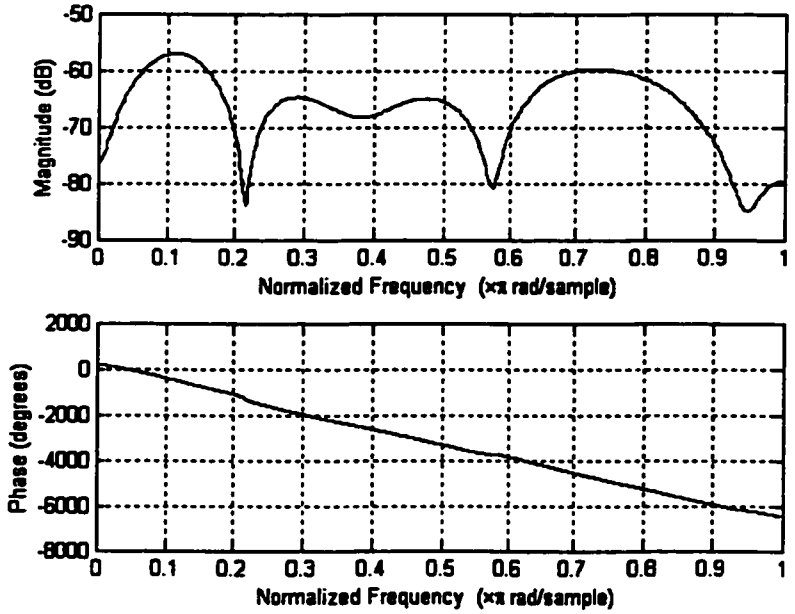

Figure 5.13 Frequency Response of the Shortened Channel

Figure 5.13 shows that the Modified MMSE method leads to a flatter frequency response of the shortened channel which maximizes the channel capacity and an almost linear phase response which leads to less phase distortion. Figure 5.14 shows the bit loading result:

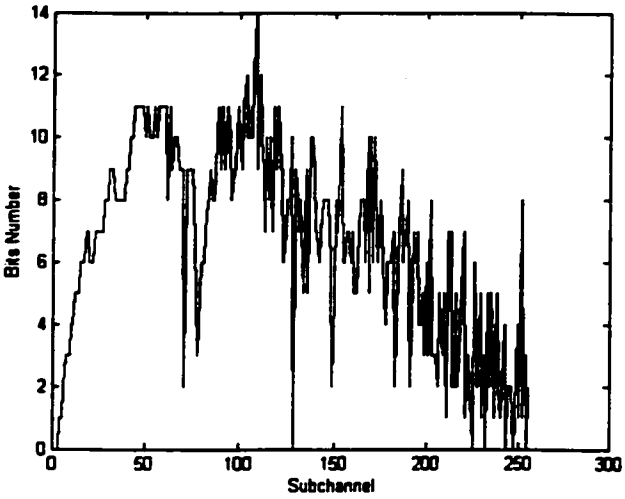

Figure 5.14 Bit Loading Result

In our simulation, it is found that even a very short TEQ designed with modified MMSE method could have a very good performance. A TEQ with 4 taps and the shortened channel impulse response is given in Figure 5.15.

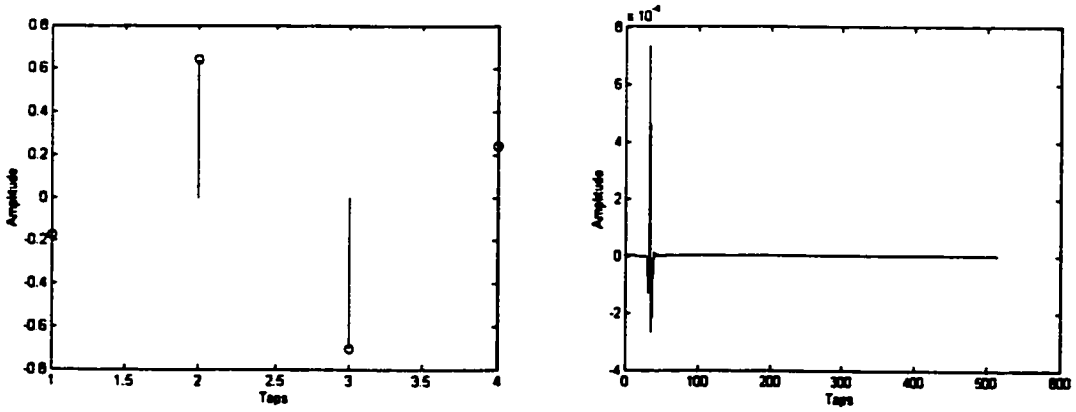

Figure 5.15 TEQ and Shortened Channel Impulse Response

Using modified MMSE method, the achieved bit rates on different CSA loops are given in the Figure 5.16.

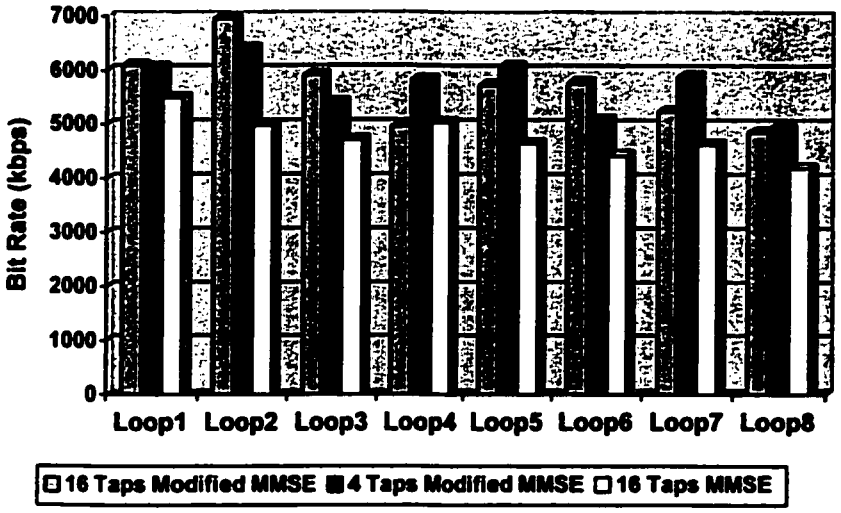

Figure 5.16 Achieved Bit Rate of Modified MMSE Method

Compared to the TEQ designed with MMSE method, the TEQ designed with modified MMSE method has a better performance and the achieved bit rate is around 1400 bits per symbol that is equal to 5.6Mbits per second.

5.3 Simulation Results of MSSNR Method

Unlike MMSE method and modified MMSE method, in MSSNR design method, the longer the TEQ, a larger SSNR can be obtained and a better performance can be achieved. In our simulation, the channel capacity is not only influenced by the ISI but also by the AGWN noise, NEXF and FEXT. Using a TEQ with 32 taps can help us to achieve a high SSNR of about 60 dB. Continuing to increase the TEQ length could result in a higher SSNR but has little influence on the channel capacity since the noise becomes the main factor that decides the channel capacity. In our simulation, we employ a TEQ with 32 taps in MSSNR design method.

Using MSSNR method, we get the TEQ with 32 taps for CSA Loop2, which is shown in Figure 5.17,

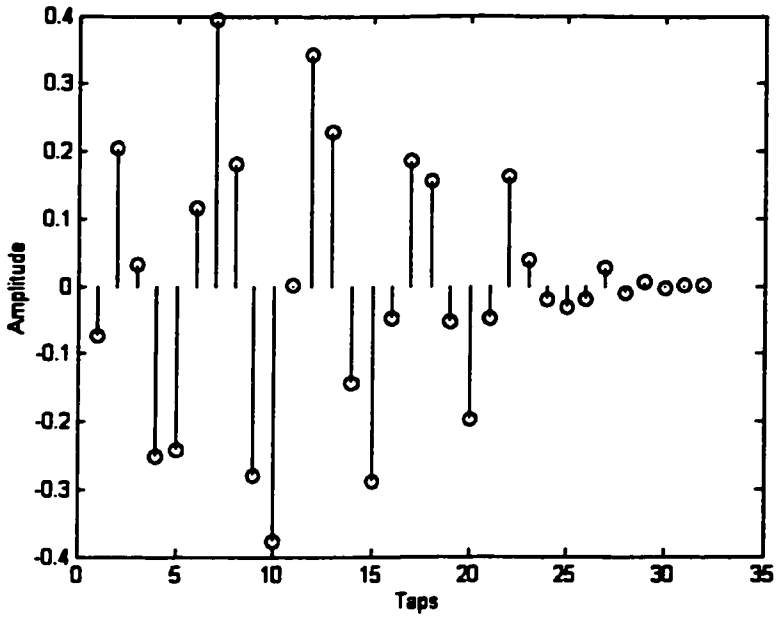

Figure 5.17 TEQ Taps Designed with MSSNR Method

The impulse response of the shortened channel is given in Figure 5.18:

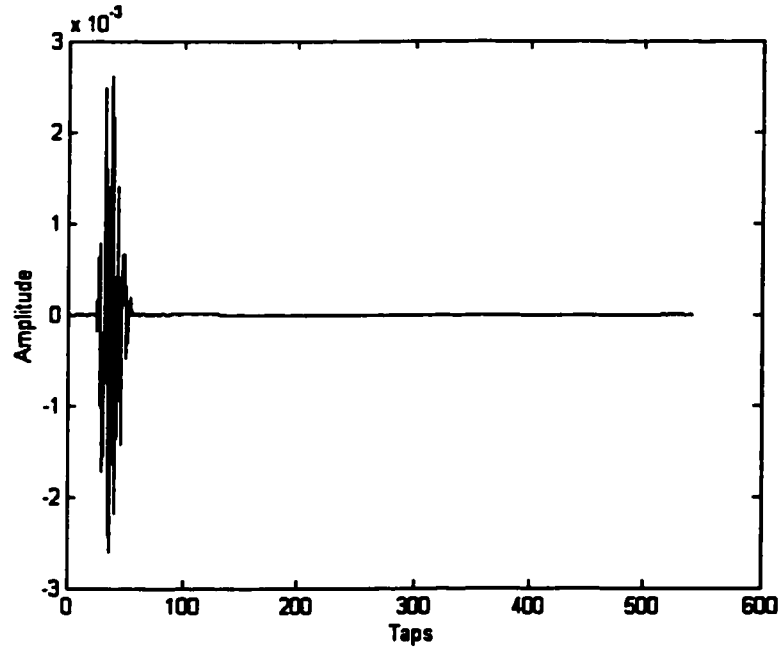

Figure 5.18 Shortened Channel Impulse Response with MSSNR Method

Comparing Figures 5.4 and 5.18, we observe that the shortened channel impulse response in Figure 5.18 is better than that in Figure 5.4. Comparing the impulse response tails in both figures, MSSNR method should have a better performance than MMSE method.

The frequency response of the shortened channel is given in Figure 5.19.

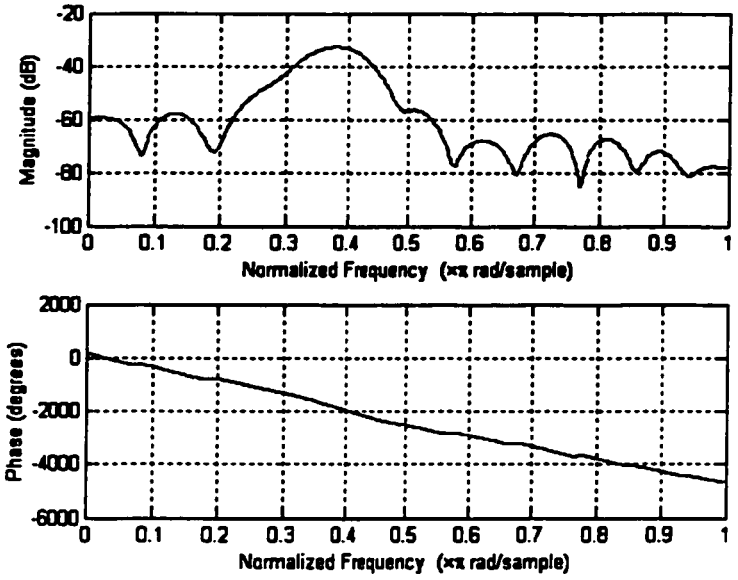

Figure 5.19 Shortened Channel Frequency Response with MSSNR Method

Comparing the frequency responses of the shortened channel obtained by MMSE method and MSSNR method, as shown in Figures 5.5 and 5.19 respectively, it is obvious that the MSSNR method leads to a flatter shortened channel frequency response.

The TEQ obtained using MSSNR method for CSA Loop3 and the shortened channel impulse response are illustrated in Figures 5.20 and 5.21.

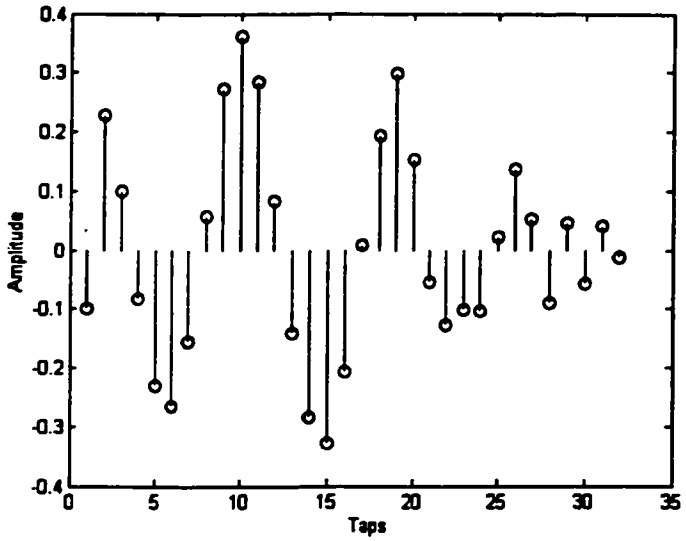

Figure 5.20 TEQ Designed with MSSNR Method

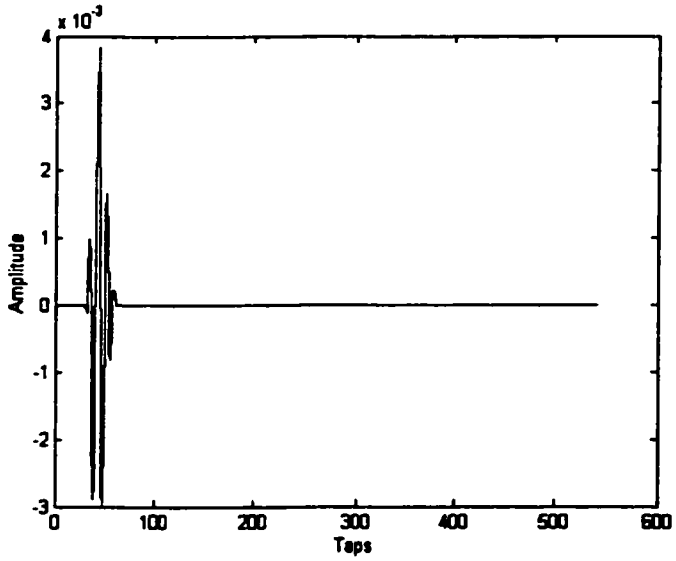

Figure 5.21 Shortened Channel with MSSNR Method

As in CSA Loop 2, we observe that the effective channel impulse response using MSSNR method is better and the impulse response energy is more concentrated. This is obvious when we measure the achieved SSNRs, which are given later.

Figure 5.22 gives the achieved bit rates using the TEQ designed by applying MSSNR method to different loops. Compared to the previous two methods, we observed that the

performance of MSSNR method is better than the modified MMSE method and is much better than the MMSE method. The achieved bit rate of MSSNR method is more than 7Mbits per second.

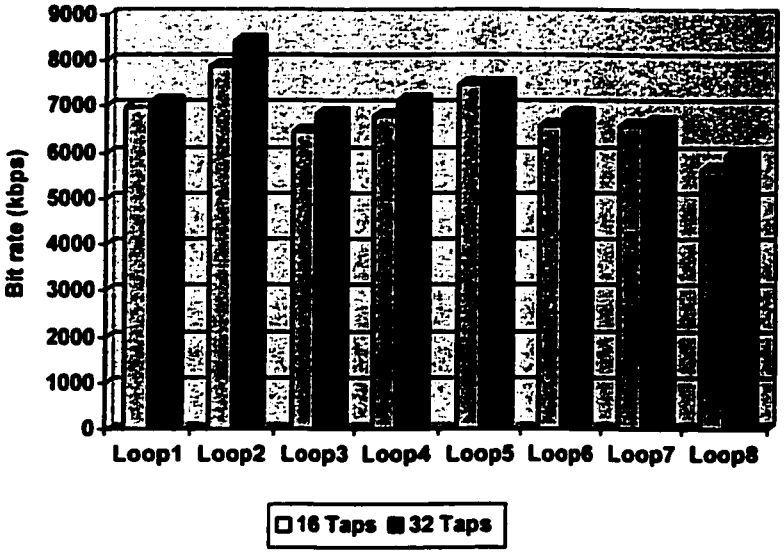

Figure 5.22 Achieved Bit Rate of MSSNR Method

5.4 Simulation Results of MRZISI Design Method

Simulation of MRZISI method is also conducted on the CSA Loops. All the CSA Loops are tested in the simulation and the detail results of Loop3 are presented here.

With the MRZISI method, a major problem is the length of the TEQ. If we use an interpolation factor of 2, according to Equation 4-19, we need to use a TEQ with more than 1000 taps, which is not practical and increases the hardware complexity. Fortunately, we found in the simulation that most of the TEQ taps is almost zero so that we could truncate the TEQ by discarding those near zero taps.

The channel impulse response of CSA Loop3 is shown in Figure 5.23.

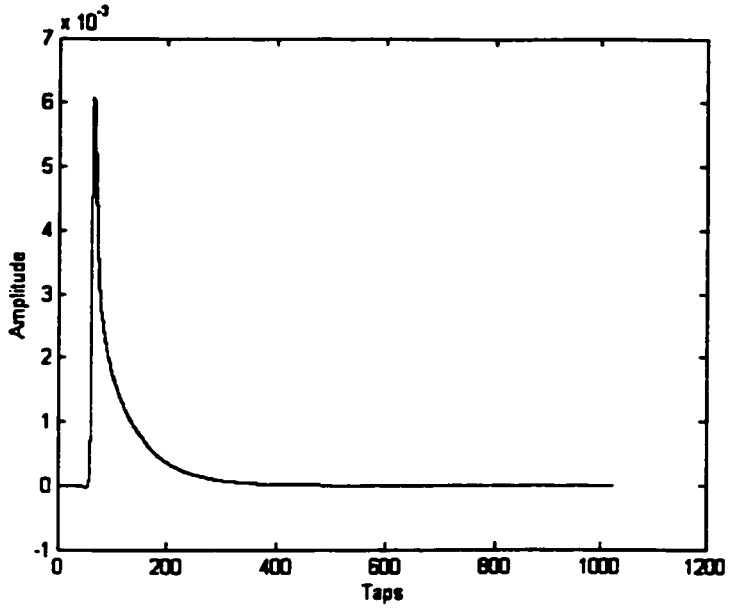

Figure 5.23 Channel Impulse Response of CSALoop 3

Using MRZISI method, we obtain the TEQ with 1024 taps as in Figure 5.24.

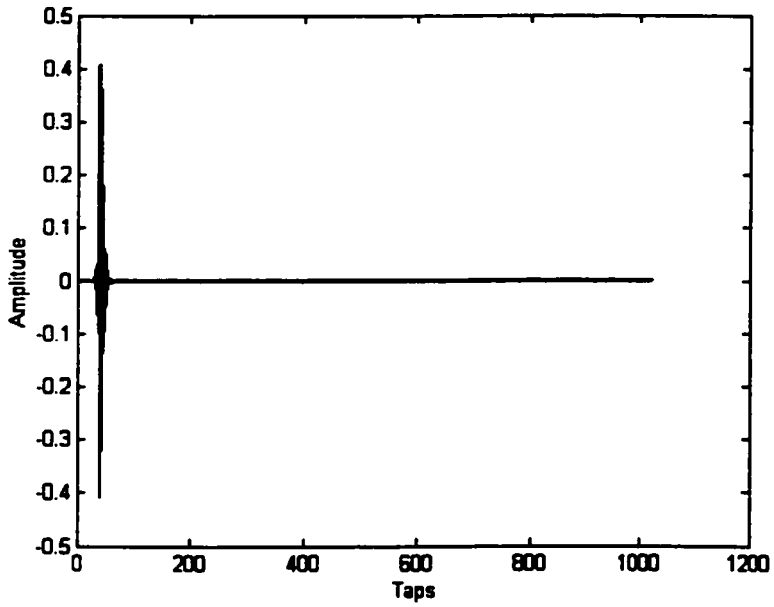

Figure 5.24 TEQ Designed with MRZISI Method

The impulse response and frequency response of the shortened channel is given separately in Figures 5.25 and 5.26.

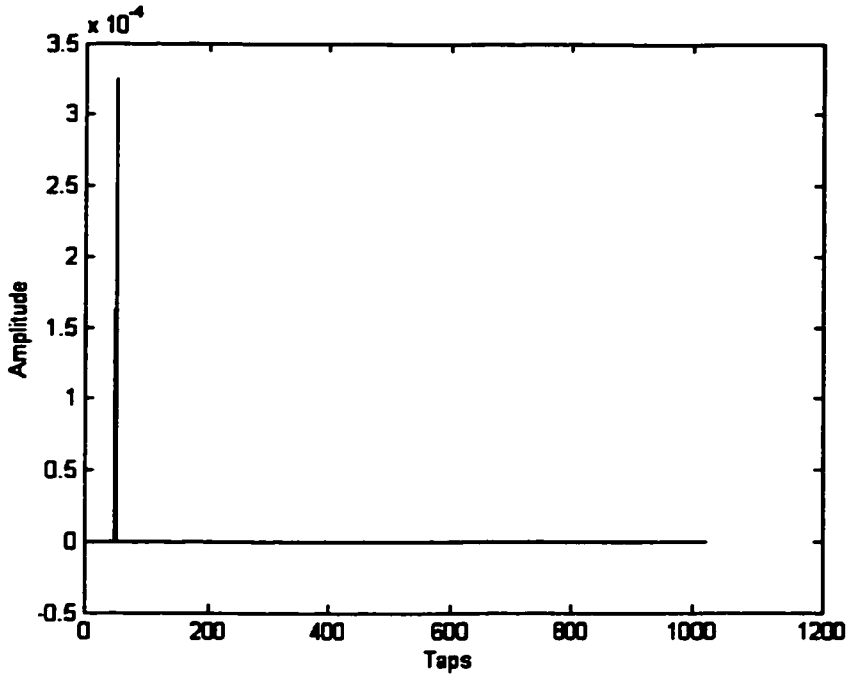

Figure 5.25 Impulse Response of the Shortened Channel

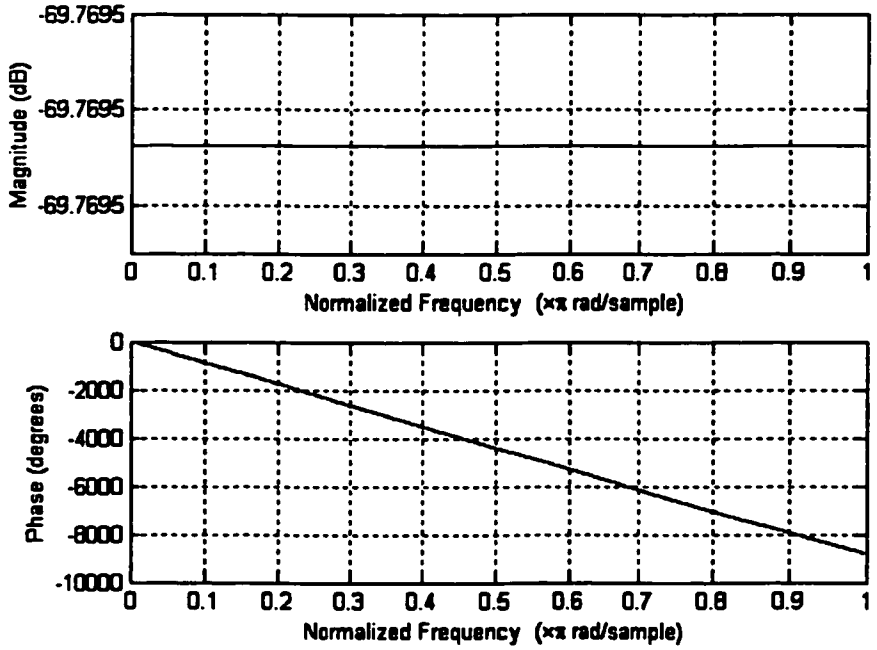

Figure 5.26 Frequency Response of the Shortened Channel

The impulse response is perfect, impulse duration is confined into one symbol and zero intersymbol interference is achieved. The channel frequency response is also perfect. It is perfectly flat and introduces no phase distortion. The SSNR achieved is tremendously high: 282.30 dB.

The only problem is that the length of the TEQ is too long and we need to truncate it. Truncation will decrease the achievable SSNR but as we discussed before, this almost has no influence on the achievable bit rate. We have two choices to truncate the TEQ: truncate the channel first and then calculate the TEQ using the truncated channel or calculate the TEQ using the original channel and then truncate the TEQ directly. From simulation, we find that the later choice has a better performance. Following is a truncated TEQ with 64 taps:

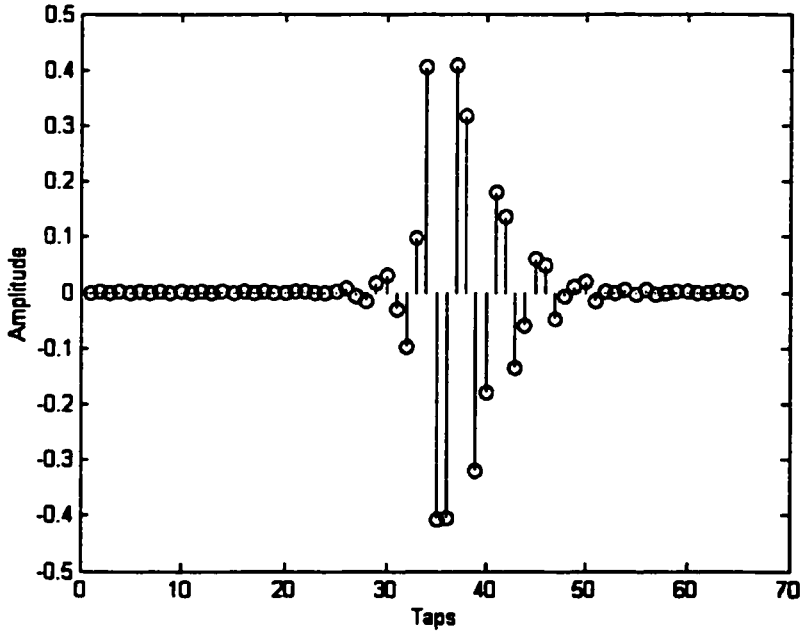

Figure 5.27 Truncated TEQ Taps

Using the truncated TEQ, the shortened channel impulse response is given in Figure 5.28,

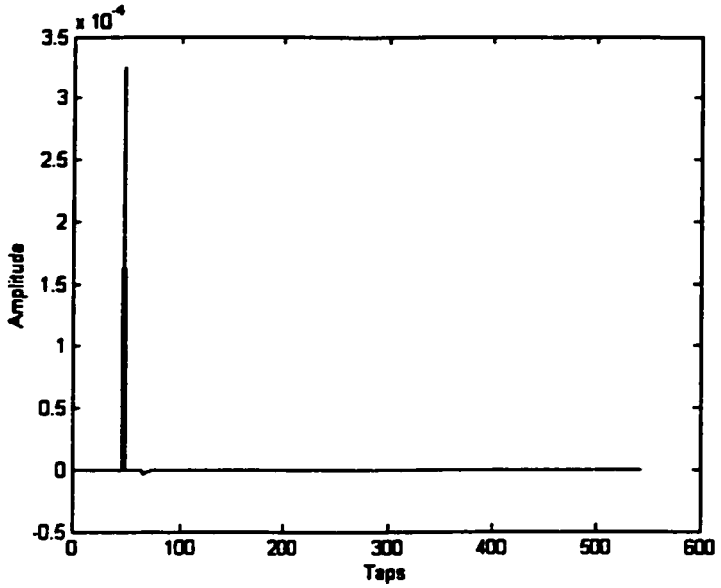

Figure 5.28 Impulse Response of Shortened Channel

We notice that the impulse response of the shortened channel is near zero ISI and there are only some very small ripples in the response. The frequency response of the shortened channel is given in Figure 5.29:

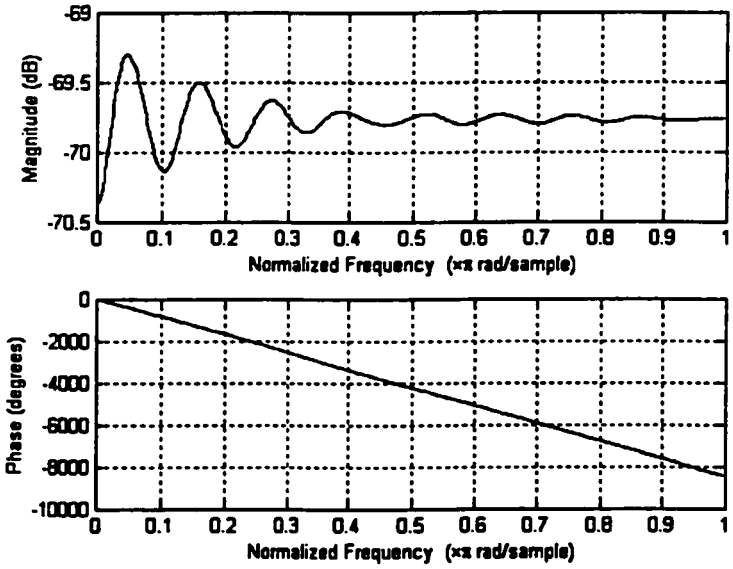

Figure 5.29 Frequency Response of Shortened Channel

The frequency response of the shortened channel is almost flat except for some small ripple. The achieved SSNR is 59.83.

Observe that there are still some near zeros in the TEQ taps; we could continue to truncate the TEQ. Following is the TEQ with 16 Taps:

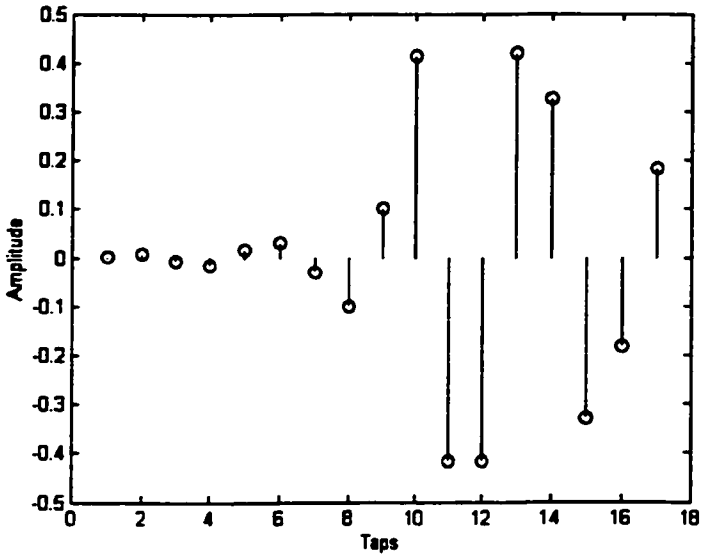

Figure 5.30 Truncated TEQ Taps

The impulse response and the frequency response of the shortened channel are given in Figures 5.31 and 5.32,

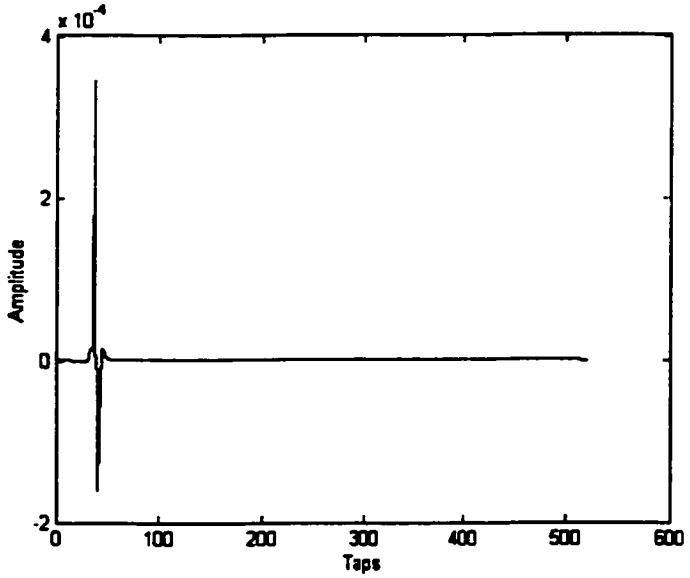

Figure 5.31 Impulse Response of Shortened Channel

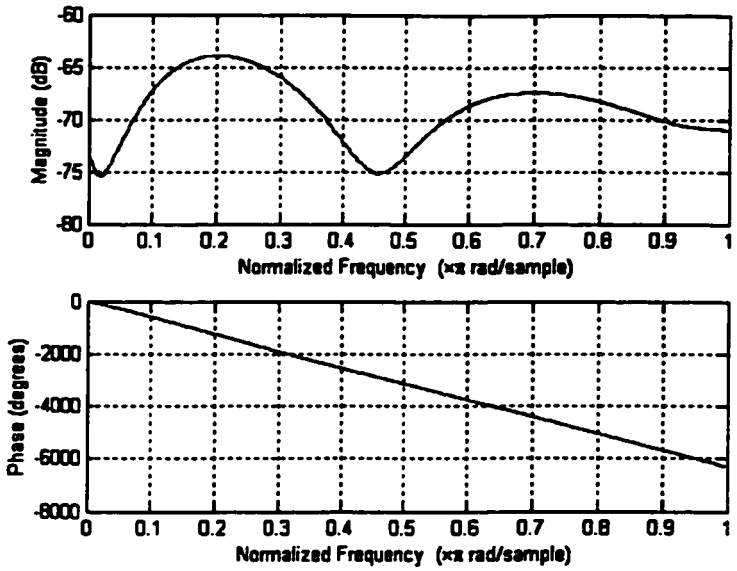

Figure 5.32 Frequency Response of Shortened Channel

It can be observed that the impulse response of the shortened channel is no longer zero or near zero ISI. But the TEQ still did a perfect job to constrain the impulse response into 32 taps and achieved SSNR of 41.07 dB which is good enough to be used in DMT system. The frequency response of the shortened channel is also good compared with the other methods. Figure 5.33 gives the bit loading result:

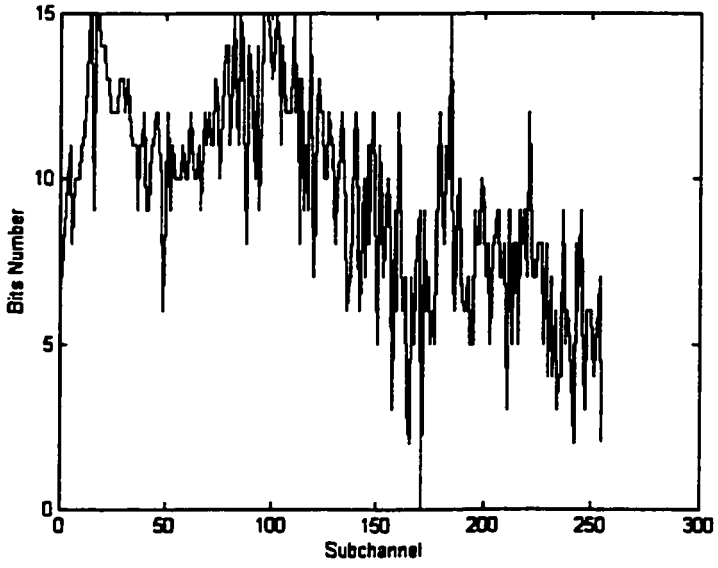

Figure 5.33 Bit Loading Result

The achieved bit rates using the TEQ (64 Taps) designed with MRZISI method on different loops are given in Figure 5.34:

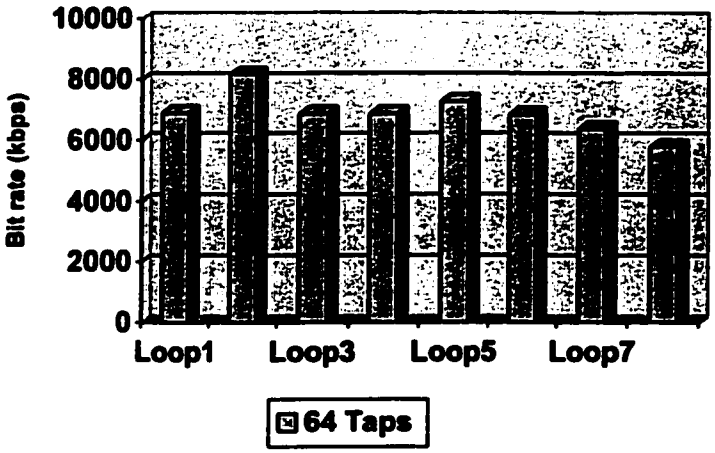

Figure 5.34 Achieved Bit Rate of MRZISI Method

The achieved bit rate on some loops is good approaching 8Mbit per second. On the other loops, the achieved bit rate is acceptable which is around 7Mbit per second.

Since the TEQ used in MRZISI method is longer than the TEQ used in other methods, especially when we need a perfect zero ISI channel where a TEQ with more than 1000 taps is required, we concern about the delay introduced by the TEQ. If the delay is too long, it may nullify the whole system. Figure 5.35 described the achieved SSNR with different delay on CSA Loop2:

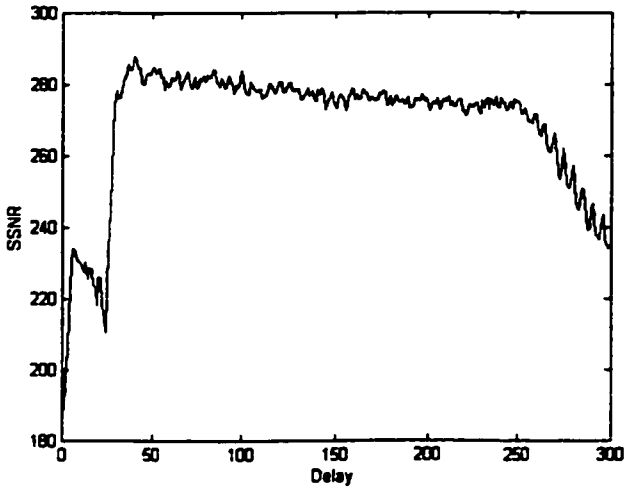

Figure 5.35 Achieved SSNR with Different Delay

It is obvious in the figure that a high enough SSNR can be achieved with a delay of about 30 taps. The delay is almost the same for other loops. Considering that the working speed of the TEQ in MRZISI method is doubled, the actual delay is roughly 15 taps. This is acceptable compared with the delay introduced by other methods (about 10 taps).

5.5 Comparison of the Simulation Results with Accurate Channel Information

In the previous sections, we showed the simulation results of the different TEQ design methods. In this section we compare all the design methods especially MSSNR method, modified MMSE method and MRZISI method.

First we take a look at the SSNR results listed in Table 5-1:

CSA Loop	MMSE 16 Taps	Modified MMSE 16 Taps	MSSNR 32 Taps	MRZISI 64 Taps
1	29.51	37.72	54.68	57.34
2	20.23	35.52	62.50	58.93
3	26.11	36.81	59.27	59.84
4	26.33	32.99	54.41	57.72
5	22.49	29.01	60.49	50.72
6	22.30	35.18	57.33	52.91
7	25.42	30.93	68.20	63.15
8	28.12	31.90	77.51	59.61

Table 5-1 SSNR of Different Methods

In Table 5-1, the achievable SSNR of MRZISI method and that of MSSNR method are around 55dB which is higher than achievable SSNR of the modified MMSE method and much higher than that of MMSE method. In fact, the SSNR of MRZISI TEQ could be infinity since the ISI is totally eliminated. In the MRZISI simulation, the TEQ is truncated in order to employ a shorter TEQ, which introduce some ISI to the system and the SNR is no longer infinity.

Since the achieved SSNR of the MMSE method is really poor, we expect that the performance of the MMSE TEQ will be poor and also the performance of the modified MMSE TEQ. The performance of the MSSNR TEQ and the MRZISI TEQ will be much better. The simulation results of the attainable bit rate are given in Table 5-2.

CSA Loop	MMSE 16 Taps	Modified MMSE 16 Taps	MSSNR 32 Taps	MRZISI 64 Taps
1	5496	6100	7100	6912
2	4992	6964	8428	8184
3	4728	5920	6856	6884
4	5040	4968	7164	6888
5	4656	5728	7504	7296
6	4436	5772	6832	6852
7	4636	5256	6672	6380
8	4196	4860	5952	5800

Table 5-2 Transmission Rate (kbps)

Figure 5.36 gives us a more direct view:

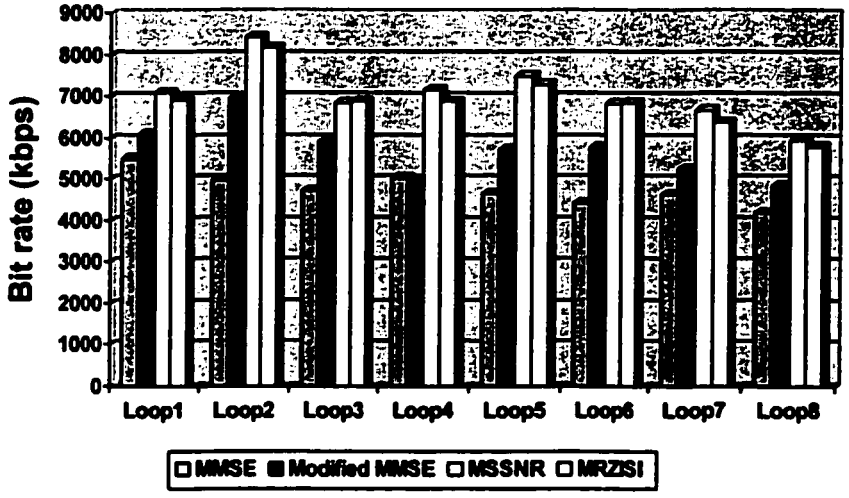

Figure 5.36 Comparison of Achieved Bit Rate of Different Methods

In Table 5-2, we notice that the transmission capacity of the MMSE method is much lower than that of the other three methods, which is less than 5Mbits per second. The transmit rate of modified MMSE method is around 1400 bits per symbol. This means we

could transmit data at the rate of 1400X4000 per second, which is about 6.4Mbits per second. The transmit rate of MSSNR method and MRZISI method is around 1800 bits per symbol, which means that we could transmit data at the rate of 1800X4000 per second, which is about 7.2Mbits per second.

It is also showed that even the SSNR of MSSNR method is higher than that of truncated MRZISI method, the transmit rate of the two methods are almost the same. In my opinion, this is because both methods have achieved a high SSNR ratio, continuing to increase SSNR will not influence the transmission rate dramatically.

Until now, all the simulations are conducted with a cyclic prefix of length 32 and all these methods could shorten the channel impulse response effectively into a time span of 32 samples. If we shorten the CP length, the MRZISI method will show more advantages.

We have explained in Chapter 4 that MRZISI method could lead to a zero ISI channel but other methods cannot. If we shorten the length of the cyclic prefix, we could expect that the performance of the MRZISI method will not change much but the performance of the other methods will deteriorate. Table 5-3 shows the achieved SSNR and transmit rate of the MMSE method, the modified MMSE method and MRZISI methods with different cyclic prefix length on CSA Loop4.

CP Length		32	28	24	20	16	12	8	4
MMSE	SSNR	26.33	23.76	14.56	14.77	12.18	7.2	-	-
	Rate (kbps)	5044	4248	2520	2520	1884	608	-	-
Modified MMSE	SSNR	32.99	29.24	25.60	21.57	17.74	11.76	5.57	-
	Rate (kbps)	4968	4900	4128	2844	2264	1004	408	-
MRZISI (256 Taps)	SSNR	69.39	69.39	69.39	69.39	69.39	69.39	69.39	69.39
	Rate (kbps)	6964	6948	7068	6936	6740	6876	6832	6868

Table 5-3 Comparisons of Different Methods with Different CP Length

From Table 5-3, It can be easily seen that the resulted SSNR of modified MMSE method and MMSE method decreased as the cyclic prefix length decreased, but the resulted SSNR of MRZISI method is almost unchanged. Adopting MRZISI method, we could

shorten the length of the cyclic prefix or even abandon the cyclic prefix that directly results in the increase of the data transmission rate by about 5%.

We could also say that the MRZISII method can deal with physical channel with longer impulse response. In a real system, the length of the cyclic prefix is fixed, but the impulse response is different from one channel to another. Some channel has extremely long impulse response. The system performance using other design methods will degrade dramatically on these channels. If we use MRZISI TEQ, the system performance will not be influenced.

Actually, the MRZISI can be used not only in DMT system but many other systems. The MRZISI could lead to a perfect zero or near zero ISI channel that is preferred in most systems, especially the frequency response of the equalized channel is linear and no phase distortion is introduced.

5.6 Simulation Results with Estimated Channel Information

In the previous sections, we compared the performances of the TEQ designed using different methods. All these results are based on the assumption that we know the channel impulse response exactly.

However, it is most likely that the precise description of channel impulse response is not available in a practical system. The channel information can be only obtained from channel estimation where the estimation error is unavoidable. There is no doubt that such kind of estimation error will influence the performance of the TEQ, as presented in the following sector.

The initialization routine of the ADSL system begins with a transmit request and several test patterns in order to make sure the channel is in operational conditions [55]. Afterwards some test patterns are exchanged, timing and synchronization is established. Then, predefined periodical pseudorandom sequences are transmitted in order to estimate

the channel transfer function and the spectral noise distribution. As the receiver knows the test sequence and its spectrum, the channel transfer function can be computed using Equation 5-1 [44].

$$H_n = \frac{1}{L} \cdot \sum_{i=1}^{L} \frac{Y_{i,n}}{X_n} \tag{5-1}$$

Figure 5.37 gives the actual channel impulse response and the estimated channel impulse response of CSA Loop 2.

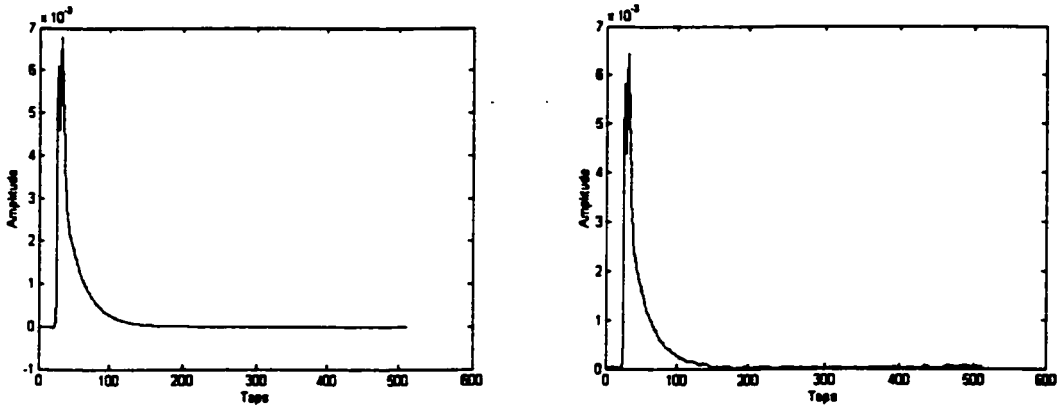

Figure 5.37 Actual and Estimated Channel Impulse Response

It is obvious on the figure that there are some estimation errors. Let's revisit the four design methods and see how such errors could influence the TEQ performance. Note that the MMSE design method does not directly use the information of the channel impulse response. Therefore, MMSE design method will not be influenced by the estimation error. The modified MMSE design method also does not use the information of the channel impulse response in TEQ design but uses the information of the channel impulse response to choose the best TEQ. The modified MMSE design method will be influenced slightly by the estimation error. In both the MSSNR and MRZISI design methods, the TEQ design is based on the information of the channel impulse response. Therefore, we expect that these two methods will suffer significantly from the estimation error.

The simulation result based on the estimated channel impulse response is given in the Table 5-4.

CSA Loop	MMSE 16 Taps	Modified MMSE 16 Taps	MSSNR 32 Taps	MRZISI 1024 Taps
1	5496	5132	2928	4828
2	4992	7056	5668	4732
3	4728	5036	2228	3576
4	5044	6172	3268	3144
5	4645	5584	4308	3192
6	4436	4296	2548	2488
7	4636	5164	2312	3180
8	4196	3564	2464	2780

Table 5-4 Transmission Rate (kbps)

Table 5-4 shows that the performances of the MSSNR design method and MRZISI design method are poorer when precise channel information is not available. The performance of the modified MMSE design method is better than MMSE method in most loops. Figure 5.38 gives us a more direct view.

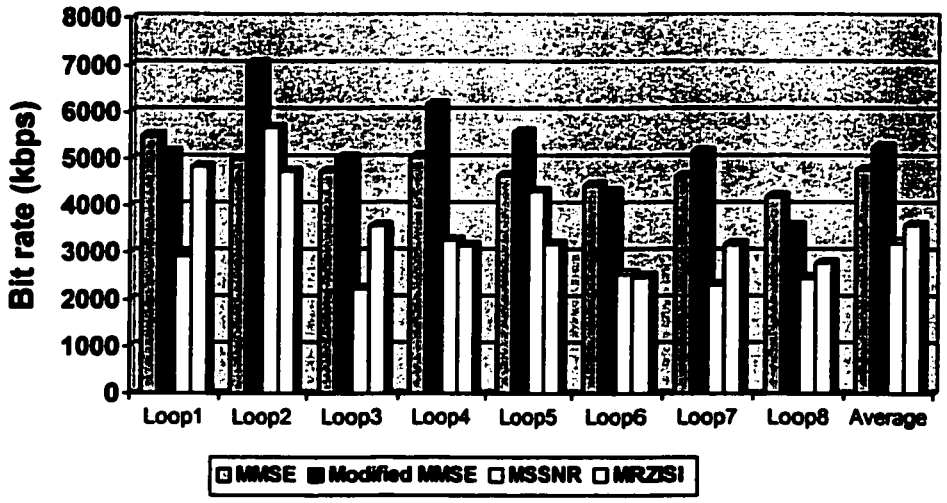

Figure 5.38 Comparison of Achieved Bit Rate of Different Methods

5.7 Additional Remarks on SSNR and ISI Shaping

In TEQ design, SSNR is used as a very important reference parameter to evaluate the performance of the TEQ. However we also notice that with the presence of estimation error, the performance of the MSSNR method and MRZISI method is really poor although the achievable SSNR is still high. Consider two cases:

Case 1: A TEQ designed with accurate channel information of CSA loop 6.
Case 2: A TEQ designed with estimated channel information of CSA loop 6.

Figure 5.39 gives the shortened impulse response of the CSA Loop 6 in case 1 where the TEQ designed is using accurate channel impulse response. The achieved SSNR in case 1 is 57.39 dB.

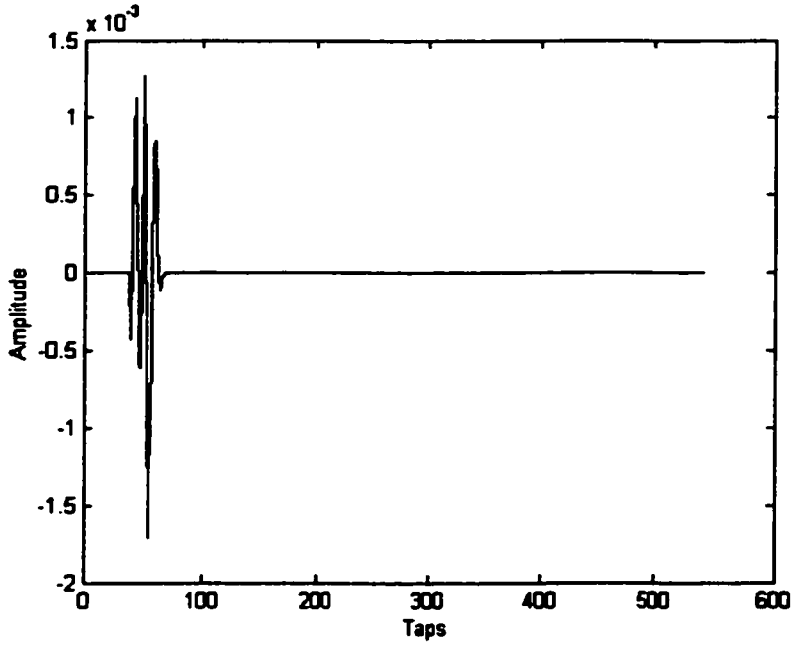

Figure 5.39 Shortened Impulse Response with Accurate Channel Information

Figure 5.40 gives the shortened impulse response of the CSA Loop 6 in case 2 where the TEQ is designed using estimated channel impulse response. The achieved SSNR is 42.96 dB.

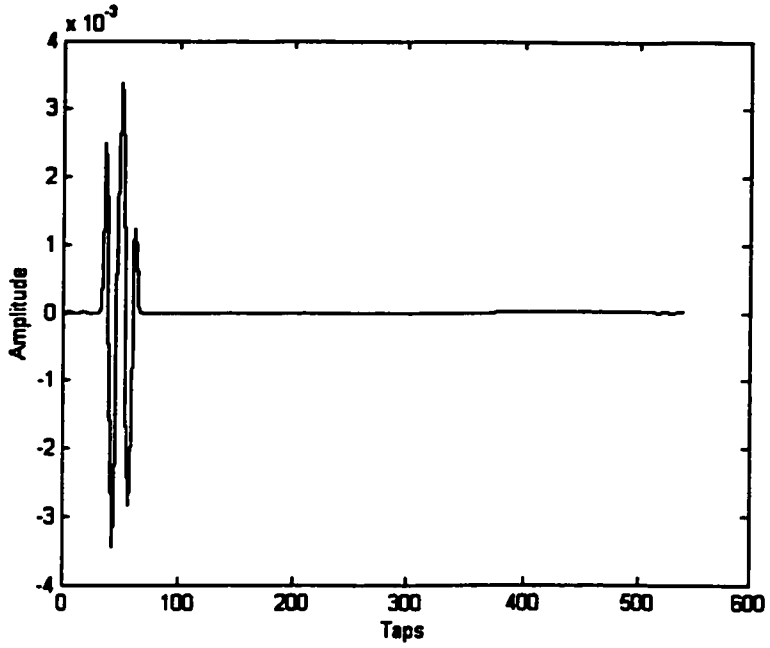

Figure 5.40 Shortened Impulse Response with Estimated Channel Information

In both cases, the effective impulse response is shortened effectively and the achieved SSNR is comparably high. But the achieved transmission rates in these two cases are different. Figures 5.41 and 5.42 give the bit loading results of the two cases respectively.

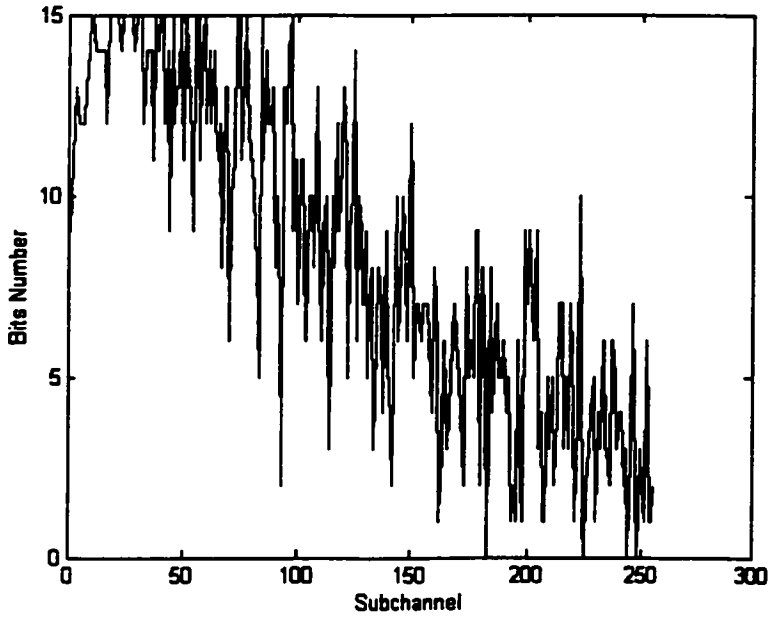

Figure 5.41 Bit Loading Result in Case 1

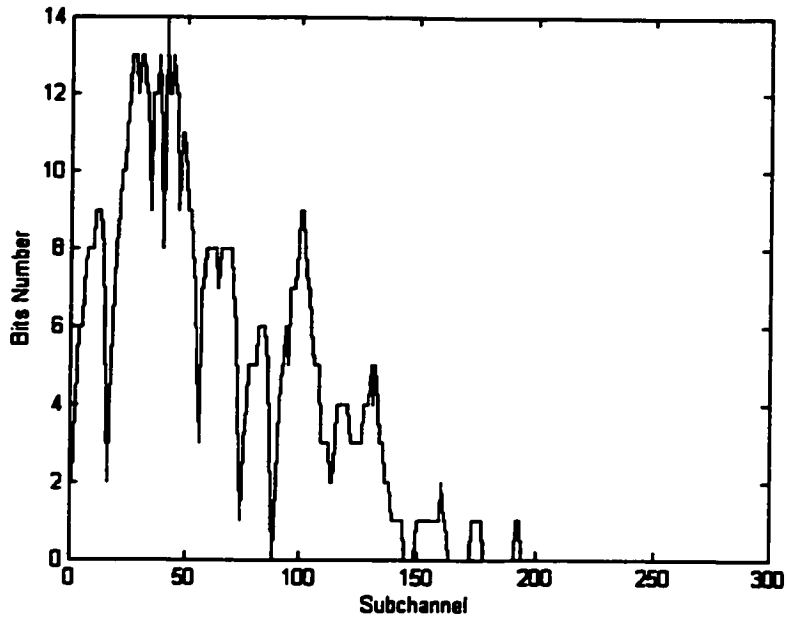

Figure 5.42 Bit Loading Result in Case 2

The achieved transmission rate in case 1 is 1700 bits/symbol and 620 bits/symbol in case 2. Further study shows that this difference results from the shape of the ISI. Figure 5.43 and Figure 5.44 give the ISI spectrum and the signal spectrum in both cases.

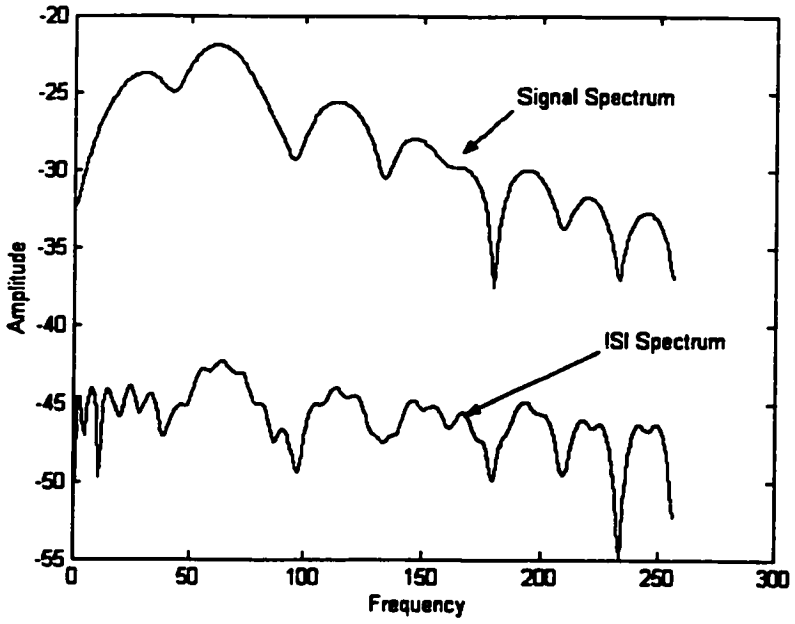

Figure 5.43 ISI and Signal Spectrum in Case 1

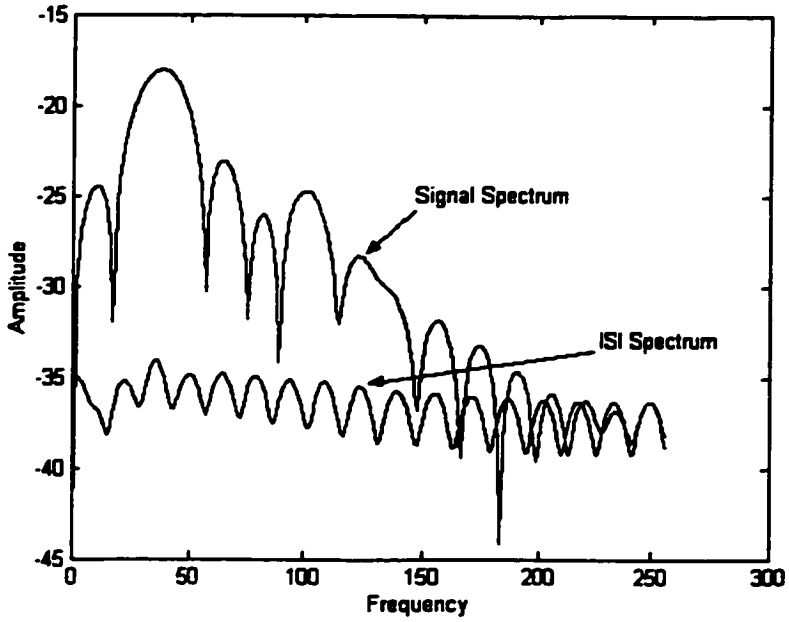

Figure 5.44 ISI and Signal Spectrum in Case 2

In case 1, we get a better ISI spectrum shape, which changes according to the changes in signal spectrum. But it fails to do so in case 2.

Comparing these two cases, we find that higher SSNR only means lower ISI power and does not guarantee higher transmission rate. Only when it is combined with a good ISI spectrum shape, high SSNR can promise a high transmission rate.

Chapter 6

Conclusions and Future Works

Conclusions:

In this thesis, we investigated various TEQ design methods in DSL transceiver system. Two prevailing design methods, MMSE and MSSNR, were discussed and compared. Two new design methods, modified MMSE method and MRZISI method, were presented and compared with two current methods. Based on the computer simulation, some conclusions are made:

1. SSNR is an important reference parameter to evaluate the performance of TEQ. Optimization of SSNR in the design method is directly related to the optimization of the channel capacity. However, the channel capacity is not only determined by the SSNR but also by ISI.

2. Compared with the other three methods, the performance of MMSE method is not satisfactory. The MMSE method minimizes the difference between the TIR and SIR, but not the impulse energy outside the TIR. This is the reason why the resulting SSNR is lower than that in the other three methods. However, the MMSE method is simple and easy to implement especially. When the accurate channel information is not available, the MMSE method is a good choice.

3. The Modified MMSE method adopts the SSNR as the criterion instead of MSE, and as a result, its performance is better than the MMSE method. It is simple and

easy to implement. The modified MMSE method is not sensitive to the accuracy of the channel information.

4. Unlike the MMSE method, the MSSNR method is trying to minimize the impulse response outside a TIR and to maximize the SSNR. This optimization leads to higher channel capacity. However, MSSNR method is complex and requires accurate channel information.

5. The MRZISI method could totally avoid the intersymbol interference and provide perfect channel response. However, it is complex and requires more FIR taps than the other methods. The MRZISI method could shorten or even eliminate the cyclic prefix. It could also combat physical channels with long impulse response. MRZISI method is robust and can be applied to many other telecommunication systems besides DSL system. But due to the numerical nature of MRZISI method, inaccurate channel information will deteriorate the MRZISI TEQ performance.

Future Works:

1. Multirate method can be also applied to MMSE and MSSNR methods. Perhaps more interesting result can be found since it is possible for us to find a design method that is not only robust and flexible but also not sensitive to estimation error.

2. Adaptive technique can be applied to multirate method.

3. Shaping the spectrum of ISI residue still needs some more research work. MRZISI method may be used to compress or extend the spectrum using different interpolation factors.

Reference:

1. S. B. Weinstein and P.M. Ebert, 'Data transmission by frequency division multiplexing using the discrete fourier transform', IEEE Transactions on Communication Technology, vol. COM-19, pp. 628-634, Oct. 1971
2. J. Proakis, 'Digital Communications', McGraw-Hill, New York, 1995
3. E. Part-Enander, A. Sjoberg, B. Melin, P. Isaksson, 'The Matlab Handbook', Addison Wesley, 1996
4. J. Proakis, 'Digital Communication', 4th Ed., McGraw-Hill Higher Education, New York, 2001.
5. J. M. Cioffi, 'A Multicarrier Primer'. Amati Communication Corporation and Standford University.
6. E. A. Lee, and D. G. Messerschmit, 'Digital Communication'. 2nd Ed., Kluwer, Boston,1994.
7. D. J. Rauschmayer, 'ADSL/VDSL Principles', Macmillan Technical Publishing, Indianapolis, 1999.
8. T. Starr, J.M. Cioffi, P. J. Silverman, 'Understanding Digital Subscriber Line Technology', Prentice Hall PTR, NJ, 1999.
9. G. D. Forney, Jr., and M. V. Eyuboglu, 'Combined Equalization and Coding Using Precoding', IEEE Communication Magazine, Page 25, Dec. 1991.
10. P. J. Melsa, R. C. Younce, C. E. Rohrs, 'Impulse Response Shortening for Discrete Multitone Transceivers', IEEE Transactions on Communications, Vol. 44, No. 12, December 1996
11. N. Al-Dhahir and J. M. Cioffi, 'Optimum finite-length equalization for multicarrier transceivers,' IEEE Trans. on Comm., vol. 44, pp. 56-63, Jan., 1996
12. J. M. Cioffi, 'very-high-speed Digital Subscriber Lines – System Requirements', ANSI Contribution T1E1.4/98-043R8, Plano, Texas, 30 Nov. 1998.

13. J. T. Aslanis, J. M. Cioffi, 'Achievable Information Rates on DSL: Limiting Information rates with Crosstalk Noise', IEEE Transactions on Communication, vol.40, No.2, pp.361-372, Feb.1992
14. P. R. Chevillat, Gottfried Ungerboeck, 'Optimum FIR Transmitter and Receiver Filters for Data Transmission over Band-limited Channels' IEEE Transactions on Communications, Vol. Com-30, No. 8, August 1982.
15. J. W. Cook, 'Wideband Impulsive Noise Survey of the Access Network' BT Technology Journal, Vol.11 No.3, July 1993.
16. Ruiz and J. M. Cioffi, 'A Frequency Domain Approach to Combined Spectral Shaping and Coding', ICC'97, pp. 1711-1715, Seattle, WA, June 1987
17. D. L. Waring, 'The Asymmetrical Digital Subscriber Line (ADSL): A New Transport Technology for Delivering Wideband Capacities to the Residence', Clobecomm'91, pp.1979-1986,1991
18. S. Davies et al., 'Australian Wideband Impulsive Noise Survey Data', ANSI Contribution T1E1.4/95-125 (Telstra), Orlando, Florida, 12 November 1995.
19. D. Fenton, 'Digital Noise Cancellation for xDSl', Thesis, SITE, University of Ottawa, 1999.
20. J.A.C. Bingham, 'Multi-carrier Modulation for Data Transmission: An Idea Whose Time Has Come', IEEE Communication Magazine, Vol. 28, no.5, pp. 5-14, 1990.
21. J. Werner, 'The HDSL Environments', IEEE Journal on Selected Areas in Communications, vol. 9, No.6, pp. 785-800, Aug.1991
22. M. Sandell, J. van de Beek, 'Timing and frequency Sychronization in OFDM System Using the Cyclic Prefix', Proceedings of International Symmposiumm on Sychronization, pp. 16-19, Essen, Germany, Dec. 1995
23. J.Garcia_Frias, 'Combined Blind Equalization and Turbo Decoding', Proceeding of ICC 99, Vancoouver, Canada, June, 1999
24. J. Garcia_Frias, 'Blind Turbo Decoding and Equalization', Proceedings of VTC'99, Houston, Texas, May, 1999
25. I. Kalet, 'The Multitone Channel', IEEE transactions on Communication, vol.37, No.2, pp.119-124. 1989

26. M. Ho, J. M. Cioffi, 'Discrete Multitone Echo Cancellation', IEEE transactions on Communication, vol.44, No.7, pp.817-825, July 1996
27. M. Ho, J. M. Cioffi, 'High speed Full-Duplex Echo Cancellation for DMT', ICC'93, pp.772-776, 1993
28. S. B. Weinstein, Paul M. Ebert, 'Data Transmission by Frequency-Division Multiplexing Using the Discrete Fourier Transform', IEEE transactions on Communication Technology, vol. Com-19, No.5, Oct. 1971
29. J. Chow, J. M. Cioffi, 'Equalizer Training Algorithms for Multicarrier Modulation Systems', ICC'93, pp.761-765, 1993.
30. J. L. Seoane, S. K. Wilson, S. Gelfand, 'Analysis of Intertone and Interblock Interference in OFDM when the length of the Cyclic Prefix is shorter than the length of the Impulse response of the channel', In Global Telecommunications Conference, volume 1, pages 32-36, 1997.
31. N. Al-Dhahir, J. M. Cioffi, 'MMSE Decision-Feedback Equalizers: Finite-Length Results', IEEE Transactions on Information Theory, vol.41, No.4, July 1995
32. E.Viterbo, K.Frazel. 'How to combat long echoes in OFDM transmission schemes: Subchannel equalization or more powerful channel coding.' Proceeding Globecomm, pp. 2069-2074, May 1995
33. B. Hirosaki, 'An Orthogonally Multiplexed QAM Systemm Using the Discrete Fourier Transform', IEEE transactions on Communications, vol. Com-29, No.7, July 1981
34. C. Tidestav, H.V. Poor, 'Joint Carrier, Phase and Frequency Offset Tracking in OFDM Systems'. EUSIPCO 2000 Tampere, Finland, September 5-8, 2000.
35. D. Landström, J. M. Arenas, J. van de Beek, P. O. Börjesson, M. Boucheret, P. Ödling, 'Time and Frequency Offset estimation in OFDM Systems Employing Pulse Shaping 'in Proceedings of the ICUPC, pp 279-283, San Diego, October 1997..
36. D. Landstrom, S. Kate Wilson, 'Symbol time offset estimation in coherent OFDM systems' COST 259 Technical Document (98)86, 6rd MC Meeting, Duisburg, Germany, Sept 1998.

37. T. Pollet and M. Moeneclaey, 'Sychronizability of OFDM Signals', In Proceedings of Globecomm'95, Vol. 3, pp. 2054-2058. Nov.1995
38. K. Sistanization, P. S. Chow and J. M. Cioffi 'Multi-tone Transmission for Asymmetric Digital Subscriber Lines (ADSL)', ICC'91, pp. 756-760, Geneva, Switzerland, May 23-26, 1993.
39. J. J. Werner, 'The HDSL Environment', IEEE Journal of Selected Areas in Communications, Vol. 9, No. 6, pp.785-800, Aug. 1991.
40. W. Y. Chen, J. L. Dixon, 'High Bit Rate Digital Subscriber Line Echo Cancellation', IEEE Journal on Selected Areas in Comm., vol. 9, No.6 August, 1991
41. J. S. Chow, J. C. Tu, J. M. Cioffi, 'A Discrete Multitone Transceiver System for HDSL Applications', IEEE Journal on selected Areas in Communication, vol.9, No.6. August, 1991
42. P. R. Chevillat, G. Ungerboeck, 'Optimum FIR transmitter and receiver filters for data transmission over band-limited channels', IEEE Transactions on Communication, vol COM-30, No.8, pp.1909-1915, Aug. 1982.
43. J. Cioffi, V.Oksman, J. Werner, T. Pollet, P. Spruyt, J. Chow and K. Jacobson, 'Very High Speed Digital Subscriber Lines', IEEE Communications Magazine, vol.37, no.4, pp.72-79, April 1999,.
44. J. S. Chow, I. Lee and J. M. Cioffi, 'Performance evaluation of a fast computation algorithm for the DMA in high-speed subscriber loop', IEEE Journal on Selected Areas Communication, vol. 13, no. 9, pp. 1564-1570, Dec. 1995
45. R. A. Gopinath, P. Steffen, P. N. Heller and C. S. Burrus, 'Theory of regular M-band wavelet bases', IEEEE Transactions on Signal processing, vol. 41, no.12, pp.3497-3510, Dec. 1993
46. K. Cheong and J. M. Cioffi, 'Precoder for DMT with insufficient cyclic prefix', Proceeding of ICC'98, Atlanta, GA, 1998
47. N. Al-Dhahir, J. M. Cioffi, 'Optimum finite-length equalization for multicarrieer transceivers', IEEE Transactions on Communication, vol.44, no.1, pp.56-64, Jan. 1996

48. G. N. Iyenngar, D. Pal, J. M. Cioffi, 'A new method of channel shortening with applications on discrete multi-tone (DMT) systems', Proceeding ICC'98, 1998

49. J. C. Tu, J. S. Chow, J. M. Cioffi, 'A discrete multitone transceiver system for HDSL applications', IEEE Journal Selected Areas Communication, vol. 9, no.6, pp.895-908, Aug. 1991.

50. J. M. Cioffi, J. Chow, J.A. Bingham, 'Equalizer training algorithm for multi carrier modulation systems', *Proc. IEEE Int. Conf. Commun.*, pp. 761-765, Geneva, May 1993.

51. S. D. Sandberg and M.A. Tzannes, 'Overlapped discrete nultitone modulation for high speed copper wire communications', IEEE J. Select. Areas Communication, vol. 13, no.9, pp.1571-1585, Dec. 1995

52. J. G. Proakis, M. A. Tzannes, M. C. Tzannes, P.N. Heller, 'DMT systems, DWMT systems and Digital Filter banks' Proceeding IEEE ICC, New Orleans, USA, 1994.

53. B. Farhang-Boroujeny, M. Ding, 'Design method for Time Domain Equalizer in DMT Transceivers', Department of E&E, National University of Singapore.

54. B. Lu, L. D. Clark, B. L. Evans, 'Fast time-domain equalization for DMT systems' 2000 IEEE Digital Signal Processing Workshop, October 15-18, Hunt, Texas, 2000.

55. M. Schlegal, 'High bit rate data transmission over the telephone loop plant, emphasizing on DMT modulation scheme' Diploma Thesis, Department of Electronics, Technological Education Institute of Piraeus